3-2023

A Comparative Analysis of Viral Aerosol Biological Sampling Efficiency of a Small Unmanned Aircraft System (Suas)-Mounted Aerosol Sampler and A Reference Static Biosampler®

Jonathan D. Moroz

A COMPARATIVE ANALYSIS OF VIRAL AEROSOL BIOLOGICAL SAMPLING EFFICIENCY OF A SMALL UNMANNED AIRCRAFT SYSTEM (SUAS)-MOUNTED AEROSOL SAMPLER AND A REFERENCE STATIC BIOSAMPLER®

THESIS

Jonathan D. Moroz, Master Sergeant, USAF

AFIT-ENV-MS-23-M-215

DEPARTMENT OF THE AIR FORCE
AIR UNIVERSITY

AIR FORCE INSTITUTE OF TECHNOLOGY

Wright-Patterson Air Force Base, Ohio

AFIT-ENV-MS-23-M-215

A COMPARATIVE ANALYSIS OF VIRAL AEROSOL BIOLOGICAL SAMPLING EFFICIENCY OF A SMALL UNMANNED AIRCRAFT SYSTEM (SUAS)-MOUNTED AEROSOL SAMPLER AND A REFERENCE STATIC BIOSAMPLER®

THESIS

Presented to the Faculty

Department of Systems Engineering and Management

Graduate School of Engineering and Management

Air Force Institute of Technology

Air University

Air Education and Training Command

In Partial Fulfillment of the Requirements for the

Degree of Master of Science in Industrial Hygiene

Jonathan D. Moroz, BS

Master Sergeant, USAF

March 2023

AFIT-ENV-MS-23-M-215

A COMPARATIVE ANALYSIS OF VIRAL AEROSOL BIOLOGICAL SAMPLING EFFICIENCY OF A SMALL UNMANNED AIRCRAFT SYSTEM (SUAS)-MOUNTED AEROSOL SAMPLER AND A REFERENCE STATIC BIOSAMPLER®

Jonathan D. Moroz, BS

Master Sergeant, USAF

Committee Membership:

Dr. Jeremy Slagley
Chair

Lt Col Casey Cooper, PhD
Member

Dr. Daniel Felker
Member

AFIT-ENV-MS-23-M-215

Abstract

Bioaerosol sampling using small unmanned aerial systems (sUAS) is a rapidly developing field that may result in a paradigm shift in emergency response and industrial hygiene sampling conventions. These technologies offer decreased sample acquisition times, larger sampling area coverage, and reduced health and safety risks to traditional human sampling teams. This potential requires a comprehensive investigation of sUAS capabilities and limitations. This study is a continuation of the characterization of an AFIT-developed sUAS-mounted aerosol sampler, proven capable of collecting viable vegetative and spore-forming bacteria through previous AFIT research. Within this study, viral biological sampling efficiency (BSE) of the sUAS-mounted aerosol sampler affixed with SKC 37 mm gelatin filter media is compared to a reference SKC Biosampler®, using Male Specific Coliphage 2 (MS2) as a model viral organism. Experimental trials were conducted within a 5.35 cubic meter, controlled aerosol test chamber using a 6-jet Collison nebulizer to loft viral aerosols. Plaque assay analysis was used to enumerate sampled MS2. Results of this study determined the mean relative BSE of the sUAS-mounted aerosol sampler to the Biosampler® in the collection of viable MS2 bacteriophage per liter of air sampled to be 4.98 (95% CI 3.9, 6.1), under these experimental conditions.

Acknowledgments

I must express my gratitude to Dr. John Tuepker. Thank you for inspiring me to take this, and any challenge head-on. I would also like to thank Lt Col Casey Cooper for imparting his bioaerosol expertise and guiding me through the development of this research. Additionally, I would like to express my thanks to Dr. Jeremy Slagley for the latitude given in completing this research and his contagious enthusiasm for small victories along the way.

Jonathan D. Moroz

Table of Contents

Page

List of Figures

Page

List of Tables

Page

List of Equations

Page

A COMPARATIVE ANALYSIS OF VIRAL AEROSOL BIOLOGICAL SAMPLING EFFICIENCY OF A SMALL UNMANNED AIRCRAFT SYSTEM (SUAS)-MOUNTED AEROSOL SAMPLER AND A REFERENCE STATIC BIOSAMPLER®

I. Introduction

General Issue

"Biological threats—whether naturally occurring, accidental, or deliberate in origin—are among the most serious threats facing the United States and the international community" (The White House, 2022). The prior passage from the most recent National Biodefense Strategy and Implementation Plan (NBSIP) was maintained verbatim from the previous 2018 version of the document. Prior to the coronavirus disease 2019 pandemic, the true scale of the potential biological threat was perhaps incomprehensible by many, apart from biological weapons and infectious disease experts. Now, these words of warning seem more palpable to a much broader audience.

The NBSIP presents a basis for this research. The document outlines 5 primary goals with objectives for each to counter these established threats. A recurring theme across the goals and objectives is innovation and time efficiency. The specific NBSIP goal on which this innovative research centers is Goal 1: "Enable risk awareness and detection to inform decision-making across the biodefense enterprise" (The White House, 2022).

From a national biodefense perspective, emergency response operations within the Department of Defense (DoD) must align with these goals. As such, the department has already described the use and advantages of sUAS remote Chemical, Biological, Radiological, and Nuclear (CBRN) sampling technologies in the Multi-Service Tactics,

Techniques and Procedures for CBRN Sampling and Reconnaissance (DoD, 2021). Furthermore, the United States Air Force has addressed the need for timely CBRN sampling within Department of the Air Force Manual 10-2503, *Operations in a CBRN Environment*:

> "CBRN agent detection and identification provide commanders the information needed to determine protective postures and to tailor protective actions to specific agent threats. Early detection provides more time to implement protective measures" (2019).

At present, time-efficient bioaerosol sampling poses a potential weak point in the initial investigative stages of a biological threat response. Under the current conventional manned response construct, procedures are in place meant to reduce health and safety risks to response personnel. These actions include health vitals checks, personal protective equipment (PPE) donning, safety briefings, and transit into the area of concern from a safe staging zone. Furthermore, responses typically are conducted in a phased entry approach, beginning with a scene 'size-up' or reconnaissance activity. For these reasons, sample acquisition alone may take many hours. In turn, analysis is then delayed, ultimately slowing data meant to support mitigative decision making. Unmanned aerial systems with onboard sampling capability provide a prospective solution. According to Eninger and Johnson (2015), there are two distinct advantages associated with these systems. The first benefit is rapid exposure assessment due to the highly mobile nature across a sampling space. The second advantage is risk avoidance for personnel collecting a sample. The authors stated these advantages in an industrial hygiene sampling context,

but they similarly apply to emergency response situations with heightened time constraints.

These imperatives led to the development of the current sUAS and mountable aerosol sampler by Ohms (2020). In addition to developing the cost-efficient, lightweight, low-power sampler, Ohms also characterized its sampling capabilities with a monodisperse aerosol. Following this, Fuller (2022) demonstrated the platform's capacity for the collection of viable spore-forming bacteria in *Bacillus thuringiensis*. The designed sampler similarly showed potential for collecting viable vegetative bacteria in *Pantoea agglomerans* (Harvey, 2022).

Problem Statement

The sUAS platform for sampling bioaerosols has been only partially characterized via vegetative and spore-forming bacteria sampling studies. Biological threats comprise other agent types including toxins and viral aerosols. Ideally, innovative bioaerosol sampling technologies such as the sUAS-mounted sampler will demonstrate versatility of sampling across these agent classes. To that end, the sUAS-mounted sampler's viral aerosol sampling capabilities, beginning with viable collection, must be studied to further clarify potential applications and limitations of the platform.

Research Objectives

The ultimate aim of this research was to further characterize bioaerosol sampling capabilities of the sUAS. Specifically, this study sought to assess the efficacy of this aerial biological sampling platform for collecting viable airborne virions. With efficacy established, the next objective was to determine comparability of the sUAS-mounted

aerosol sampler's viable sampling efficiency to traditional and proven bioaerosol sampling equipment. This was accomplished by ascertaining the mean relative BSE (with 95% confidence interval) of a filter-based sampler affixed to the sUAS (in simulated flight) against the reference SKC Biosampler® using MS2 bacteriophage as a surrogate pathogenic virus.

Investigative Questions

The prerequisite question prior to obtaining a relative BSE was assessing whether the sUAS-mounted sampler was capable of sampling a viable airborne virus with gelatin filters as a selected media. Based on affirmative results to the former, the second question posits how comparable sUAS-collected viable concentrations were to those of a well characterized, viral aerosol reference sampler.

Methodology

As with previous studies within this line of sUAS research, all sampling trials were conducted in the Multi-Use Research for Particulate Hazards and Exposure Environment (MURPHEE) test chamber. MS2 bacteriophage was aerosolized using a Collison nebulizer, after which concurrent air samples of the sUAS-mounted sampler and Biosampler® were collected over 30 trials. Samples were then transported to AFIT laboratories for analysis via plaque assay.

Plaque assay results yielded viable virus concentration in plaque forming units per milliliter (PFU/mL). Next, measured post-sampling liquid volumes of the Biosampler® and gelatin filter solution (in mL) were used to ascertain total PFU in each sample. These values were then divided by the total air volume collected (in L) for each given sample

(corrected for standard temperature and pressure) to obtain PFU/L. Comparable, by-trial ratios of PFU/L concentrations sampled by each device were then used to determine the mean relative BSE (with the Biosampler® as a reference point of 100% efficiency). A 95% confidence interval surrounding the mean relative BSE was calculated. Lastly, a Wilcoxon Signed-Rank test was performed to test the difference in means via the relative BSE ratio. The null hypothesis of this research states the mean BSE will be equal to 1, indicating no difference between the two samplers. The alternative hypothesis states the mean BSE will not be equal to 1.

Assumptions/Limitations

Limitations of this study largely pertain to the laboratory conditions in which samples were obtained. Relative humidity within the aerosol chamber was uncontrolled and may not have been reflective of ambient outdoor levels. Furthermore, air velocity within the chamber was a very low 0.2 m/s (0.38 knots). This air velocity would equate to ideal calm wind conditions for outdoor sampling. Under these favorable conditions, the sUAS hover would be more stable, conceivably preserving battery life and being closer to isokinetic sampling than would higher wind speeds.

Power sources for the sUAS and the onboard sampling fan were both external for this research. Field sampling would require an onboard battery capable of powering both systems for up to 15 minutes, if replicating sampling methodologies. Weight contributions of an onboard battery capable of powering both the sUAS and the sampler were evaluated and found to be well within technical performance measures (Ohms, 2020). Moreover, the power draw from the sampling pump was a negligible contribution

to the overall sUAS power consumption. Most notably, battery-powered endurance of the platform was estimated for both flight and sampling, finding 19 minutes of operable run-time (Ohms, 2020).

Implications

The results of this study contain evidence which may support the increased use of unmanned sampling equipment for DoD biological responses. Should field studies involving the sUAS as a bioaerosol sampling platform demonstrate similar utility in collecting viable bioaerosols as those in more controlled settings, the sUAS could prove to be a versatile response capability.

Moreover, concurrent remotely controlled aerial reconnaissance and sampling of a suspected biological agent hot zone could drive a rethinking of response operations conventions. Deployment of the sUAS could significantly reduce human safety related procedural delays. Furthermore, sUAS operators could be located in a proximal zone, but away from areas of concern. Consequently, response personnel health risks could be reduced with this technology in environments conducive to its use. In summary, sUAS-mounted bioaerosol samplers have the potential to radically change the current approach to biological response operations. Short of this, they may offer a remote sampling capability that supplements current DoD biological response equipment assemblages.

II. Literature Review

Chapter Overview

The goal of this study was to continue the line of research on the sUAS-mounted sampler developed by Ohms (2020) and assess airborne viral BSE relative to a reference sampler. This chapter seeks to assess relevant literature pertaining to viral aerosol sampling employing an sUAS. To the best of this author's knowledge, the current study represents novel research in the field of active viral sUAS platform sampling, as other work in this space utilizes passive sampling methods. The primary goals of this chapter are to find recurrent themes and trends in the literature for static and aerial bioaerosol sampling research. The topics covered within this review include sUAS application for the sampling of bioaerosols, surrogate selection, aerosolization methods, sampling devices, and analytical techniques.

sUAS Sampling of Bioaerosols

The sUAS has proven to be an effective platform for collecting airborne environmental samples where manned aircraft are impractical or infeasible. Recurring themes in these environmental studies include the sampling of air pollution, both generally (Rohi et al., 2020), and for more specific analytes such as particulate matter (Hedworth et al., 2021; Li et al., 2020) and greenhouse gases (Schuyler & Guzman, 2017). The more niche environmental standoff sampling of bioaerosols using sUAS platforms has been studied to a lesser degree. However, there are several innovative designs that have been successfully trialed for diverse applications in the scientific literature.

Biology researchers seeking to characterize respiratory microbiomes of cetaceans have employed custom-designed unmanned aircraft systems with mounted bioaerosol samplers (Centelleghe et al., 2020; Geoghegan et al., 2018; Pirotta et al., 2017). These studies all used passive sampling to capture blow spray bacteria and viruses on nutrient agar media. Pirotta et al. (2017) and Centelleghe et al. (2020) attempted to identify bacteria via 16S ribosomal ribonucleic acid (rRNA) sequencing. Geoghegan et al. (2018) represented novel research in utilizing the sUAS platform to sample airborne viruses. The authors of this study noted a challenge with low RNA concentrations from individual samples using the passive nutrient agar approach which precluded identification through sequencing. Thus, 19 samples were pooled and concentrated to enable identification. The sUAS design in the cetacean microbiome studies was stated to address challenges with accessibility, safety, and cost (Pirotta et al., 2017). These themes likewise extend to biological agent sampling applications.

An sUAS-mounted sampler has also been used to sample bioaerosols over aquatic bodies (Powers et al., 2018). Passive sampling onto agar plates was also used to collect various bacteria and fungi present over freshwater and marine environments. The study's analysis included simple quantification of total colony-forming units without differentiation.

Several studies have explored the use of sUAS-mounted biosensors for rapid bioaerosol detection. Palframan et al. (2014) sought 'near real-time detection' via biosensors onboard a fixed wing sUAS. Within this study, researchers utilized a liquid impinger coupled with a surface plasmon resonance biosensor. The equipment package was also capable of relaying measurements to ground-based receivers. The direct

measurement component was in addition to onboard Petri plates for follow-on laboratory analysis. This sUAS design contrasts the majority of those found in the literature as it remotely sampled, concentrated, analyzed, and relayed in-flight measurements. Testing of similar instrumentation on a rotary sUAS presents an area yet to be studied.

Bioaerosol sampling with a rotary sUAS-mounted sampler diverges from static bioaerosol sampling in several regards. Firstly, weight limitations exist for aerial sampling devices to allow for flight. This restricts the selection of bioaerosol samplers to lightweight equipment, namely filters. Secondly, stresses associated with flight are a factor—namely for mounted samplers with open-face designs. These additional stresses include increased airflow from rotor wash and air resistance or drag forces associated with flight. Faster moving air across a filter media coupled with air pulled through the filter could cause desiccation or drying of the filter depending on the media type (Harvey, 2022). Turbulent airflows caused by flight are also prohibitive of isokinetic sampling, and likely to cause negative biases or under-sampling of the target bioaerosol (Ohms, 2020). The associated limitation is not capturing sufficient concentration of the target bioaerosol for identification and/or quantification. The limitation becomes amplified when the analytical technique requires the collected bioaerosol to be in a viable state. Harvey (2022) observed this phenomenon while seeking to quantify viable *Pantoea agglomerans* bacteria after sUAS sampling with gelatin filters. Inconsistent detections and low concentrations precluded quantification during sample analysis. These outcomes appear partially attributable to the desiccation of sample media and organism dehydration caused by sUAS rotor wash. The hardier spore-forming bacteria, *Bacillus thuringiensis*, proved quantifiable when collected on a filter medium affixed to the sUAS (Fuller, 2022).

Airborne virions by family will also demonstrate a range of resistance to sampling-related stresses. Selecting the appropriate analytical techniques for viral aerosol samples may be of higher consequence as limits of detection can vary greatly and viability of the sampled organism is not always a necessity. These topics will be discussed in more detail in the *Analytical Methods* section. In addition to this factor, considering the dearth of sUAS viral aerosol sampling research, applying a thoroughly studied and hardy surrogate may better elucidate research questions.

Surrogate Selection

Researchers have used MS2 bacteriophage extensively as a viral surrogate since the mid-twentieth century. Some studies ascribe MS2 as a model for a select organism that would otherwise be infeasible to study directly, while others apply its surrogacy to represent more generally across the virus taxon. Diverse research topics involving the use of MS2 demonstrate its versatility. These include fomite (Brady et al., 2017), filtration (Bałazy et al., 2006; Fisher, Richardson, Harpest, Hofacre & Shaffer, 2012; Eninger et al., 2008), and disinfection studies (Sassi, Reynolds, Pepper & Gerba, 2018; Chen et al., 2022). The selection of MS2 bacteriophage as a surrogate for a given study is multifactorial and oft dependent on the nature of the research. Recurrent selection rationale for aerosol studies which constitutes further inquiry includes relative safety and morphology.

Reduced health risk is a practical justification for use of a surrogate organism. Examples of pathogenic target organisms for which MS2 is employed as a surrogate include norovirus (Dawson, Paish, Staffell, Seymour & Appleton., 2005; Tung-

Thompson, Libera, Koch, Reyes III & Jaykus, 2015), Ebola virus (Sassi, Reynolds, Pepper & Gerba, 2018; Lin & Marr, 2017), and Newcastle disease virus (Turgeon, Toulouse, Martel, Moineau & Duchaine, 2014). Often, as with the aforementioned studies, researchers experimentally introduce MS2 as an aerosol. Aerosols of the target pathogenic organisms would present unnecessary risks during experimentation and require heightened Biological Safety Level precautions (Centers for Disease Control and Prevention, 2020). Known pathogenic risks and associated control measures invariably add cost, oversight requirements, and time to viral studies. Thus, MS2, and bacteriophages in general, are frequently selected as surrogates for viral aerosol research due to their benign nature with respect to human health.

According to Nayak (2011), viral morphology comprises characteristics such as size, shape, and physical features (e.g., envelope), but is principally characterized by the structure of the capsid and the presence or absence of an envelope (p.79). A viral envelope refers to a lipid bilayer acquired from infected host cell structures designed to protect the viral genome (Lenard, 2008). MS2 is a non-enveloped virus with a single strand ribonucleic acid (RNA) genome. These features denote classification as a Baltimore Class V virus (Marintcheva, 2018). Furthermore, the absence of an envelope has been observed to make virions more resilient to environmental stresses like pH and relative humidity than enveloped viruses (Lin, Schulte, & Marr, 2020).

Another commonly cited surrogate selection factor in viral aerosol studies is the size of the target organism virion relative to the surrogate organism virion (Tung-Thompson, Libera, Koch, Reyes III & Jaykus, 2015; Hogan et al., 2005). Size of viral aerosol particles has empirical implications on bioaerosol studies, namely settling rate

and sampling efficiency (Cooper, 2010). Moreover, health effects from bioaerosols are said to be size-dependent (Hogan et al., 2005). However, the size of viral aerosol particles is less determined by virion size, but by the aerosolization medium and aerosol generation method (Hogan et al., 2005). To this point, the authors evaluated the influence of viable virus presence in a medium on particle size distributions. They accomplished this by characterizing and comparing size distributions for total particles and particles containing viable viruses. The authors noted the total particle size distribution was significantly greater than that of particles containing viable virus, suggesting the presence of viruses in the suspension had an insignificant impact on the size distribution (2005).

Another important morphological aspect of bacteriophages, significant to bioaerosol sampling is the presence or absence of a tail. Verreault, Moineau, and Duchaine (2008) explain this as a key limitation in early studies of infectivity using tailed phages as surrogate organisms. The tails of Caudovirales order bacteriophages used in such studies are important for host recognition, attachment, and subsequent infection (Dubovi Amn & Akers, 1970). Thus, should the tails become compromised from physical stresses associated with aerosolization, the surrogate cannot reliably determine the resulting infectivity (Verreault, Moineau, and Duchaine, 2008). Leung et al. (2019) drew a similar conclusion from their work where three different tailed phages were analyzed by transmission electron microscope for the presence of morphological changes resulting from jet nebulization. The study confirmed morphological changes indeed resulted from these physical stresses and correlated the changes to losses in infectivity.

More broadly, tailed phages may be unsuitable as surrogates for viruses that infect eukaryotes. Turgeon, Toulouse, Martel, Moineau, and Duchaine (2014) argue that despite

tailed phage usage being predominant in the literature for a wide array of study types, the tailed feature renders them inappropriate for comparison to viruses infecting eukaryotes, which are absent tails. Thus, it stands to reason there should be a shift to tailless phage surrogate selection for aerosol studies which measure infectivity and/or seek to model specific pathogenic target viruses affecting eukaryotes. This logic notwithstanding, studies using tailed phages for aerosolization are ongoing. However, it has become more standard to use multiple surrogate organism types to reduce bias and draw stronger conclusions (Jang, Bhardwaj & Jang, 2022; Hong, Bhardwaj, Han & Jang, 2016). Within these works, the authors acknowledge that the fragility of tailed phages makes them better suited for comparison to likewise fragile target viral organisms. No overt disclaimers such as these surround the surrogacy of MS2, though the principle of applying any surrogate to an appropriate target organism is fundamental to this discussion. In summary, when selecting a suitable surrogate, researchers should consider many factors not limited to risk and morphology.

Aerosolization Methods

As mentioned in the previous section, methods of viral aerosol generation have significant effects on particle size distribution which in turn affects sampling efficiency (Hogan et al., 2005). Thus, the selection of the appropriate aerosolization method is crucial for study design. There exist only a small number of well-characterized aerosolization methods for bioaerosols. Hogan et al. speak to a primary technology—the Collison nebulizer—used "almost exclusively" (2005). This literature review similarly observed the predominant use of this aerosolization device for MS2, in both 3-jet (Tseng

& Li, 2005; Hong, Bhardwaj, Han & Jang, 2016; Jang, Bhardwaj & Jang, 2022) and 6-jet (Bałazy et al., 2006; Fisher, Richardson, Harpest, Hofacre & Shaffer, 2012; Eninger et al., 2008) variations. The Collison nebulizer was invented in 1932 and used within the research community for various applications but quickly became a staple within microbiology studies (May, 1973). May describes the mode of operation as follows: compressed air is forced through to the nozzle which creates a drop in static pressure. The resulting drop draws liquid from the reservoir. The liquid is then dispersed by way of the airstream into aerosolized droplets having a wide size distribution. The sampler retains over 99 percent of the droplets via collision and accumulation on the internal wall, which returns the liquid to the reservoir. The tiny fraction of aerosol escaping the sampler to the exterior air makes up the "finest tail of the drop-size distribution" (1973). The aerosols are then subject to the atmosphere where relative humidity determines the rapidity of droplet nuclei formation. May (1973) states:

> "If the drops in this emerging aerosol are aqueous, or of some other volatile liquid, they will evaporate very rapidly on admixture with unsaturated air. For example, a 10-micrometer water drop in air at 20°C and 80 percent relative humidity has a wet lifetime of 0.6 sec."

Hogan et al. describe this droplet nuclei formation phenomenon after aerosolization from the Collison nebulizer as exhibiting a "time-varying size distribution" (2005). The fluctuating size distribution may have direct effects on sampling efficiencies, assuming the aerosols do not reach equilibrium by the time they reach the sampling device.

Atomizers have also been used in viral aerosol studies (Turgeon, Toulouse, Martel, Moineau & Duchaine, 2014; Dubovi Amn & Akers, 1970; Hogan et al., 2005).

The mode of operation begins similarly to a Collison nebulizer in that a pressure drop via introduced compressed air is also used to draw liquid from a reservoir up into an airstream. The technologies differ as the atomizer employs a capillary through which small aerosols are generated versus dispersion of the liquid via the airstream itself, as with the Collison.

In the Hogan et al. (2005) study, the authors noted the size distribution produced by the atomizer was not time-varying as observed for the Collison. The use of a diffusion dryer prior to the analysis of the particle size distribution may explain this result. As such, the conclusion of the atomizer not producing a time-varying size distribution becomes less consequential as the atomizer may not have been the sole variable responsible for the change. An improvement to the Hogan et al. study design would involve similar use of the diffusion dryer for both aerosolization mechanisms prior to particle size distribution characterization.

Hogan et al. (2005) found viable MS2 in similar concentrations from aerosolization via the Collison nebulizer (no diffusion dryer) and the atomizer (with diffusion dryer). This conclusion is questionable due to the incorporation of the diffusion dryer in only 1 of the aerosol-generating devices. A later study by Turgeon, Toulouse, Martel, Moineau, and Duchaine (2014) again evaluated viability of MS2 after aerosol generation through both a Collison nebulizer and atomizer, each with a diffusion dryer in-stream. These findings suggest negligible differences in viability losses between the atomizer and Collison nebulizer. Researchers in this space should evaluate the effects of diffusion dryers on viability for several phage types, including MS2, to support the continued usage in bioaerosol studies.

Several lesser-used technologies have also appeared in the literature. These include ultrasonic atomizers of varying frequencies. Dybwad, Skogan & Blatny (2014) aerosolized MS2 at 48 kHz, while Ratnesar-Shumate et al. (2015) used a 120 kHz nozzle. The authors do not adequately explain the chosen frequencies within these studies, but they are presumed to correspond to a desired mass median aerodynamic diameter (MMAD). These uncertainties warrant a particle size distribution characterization of these devices at differing frequencies as well as an evaluation of potential viability losses for confidence of use in viral aerosol studies. Lastly, Eninger et al. (2009) evaluated an electrospray against a Collison nebulizer for producing MS2 aerosols. The authors observed the electrospray to produce a more monodisperse aerosol and twenty times higher viable airborne concentrations relative to the Collison nebulizer. These devices are applicable when electrostatic charges of bioaerosol particles are a consideration, though they may be cost-prohibitive.

Foaming from media agitation within the aerosolization device presents a potential difficulty for bioaerosol studies. Excessive foaming will cause disruptions to liquid flow through to the nozzle of the Collison nebulizer and reduced capillary diffusion for atomizers. This effect in turn causes changes in the particle size distribution of the outgoing aerosol streams. The type of liquid media selected may have pronounced foaming effects. For example, an organic liquid derived from eggs found to preserve certain phage types was not suitable in the Collison nebulizer due to excessive foaming and clogging (Turgeon, Toulouse, Martel, Moineau & Duchaine, 2014). Viral propagation media may undergo additional treatment, including centrifuge or dialysis, to reduce foaming effects (Hogan et al., 2005). Additionally, researchers often dilute viral

suspensions with an inert liquid such as sterile deionized water prior to aerosolization to obtain the desired starting concentration lower than that of the propagation titer. The described dilution process offers the added benefit of reducing foaming. Thus, MS2 aerosol studies seldom cited the use of additional chemical antifoam agents during this literature review.

Sampling Devices

Viral sampling devices fall under the broad equipment categories of impingers, cyclones, filters, and impactors (Chandler et al., 2017). Flight limitations (e.g., weight and turbulence) within the present study preclude the selection of certain sampling devices, such as those using liquid media or samplers weighing more than several ounces. Additionally, previous lines of research with the present model sUAS successfully sampled for Arizona Road Dust (Ohms, 2020), vegetative bacteria (Harvey, 2022), and spore-forming bacteria (Fuller, 2022) using a filter-based sampler. Thus, this study compares the relative efficiency of a reference static liquid impinger employing the Biosampler® (SKC Inc., Eighty-Four, PA, USA) against an sUAS sampler affixed with 37 mm gelatin filters (SKC Inc., Eighty-Four, PA). Topics addressed within this chapter germane to these devices include physical sampling efficiency (PSE), preservation of viability, environmental condition effects on performance, and collection and extraction media.

The selected reference sampler, the Biosampler®, is an improved liquid impinger device, optimizing the design of the All Glass Impinger (AGI) -30. The Biosampler® similarly collects bioaerosols into a liquid collection medium, but does so by swirling the

in-going aerosol stream and the collection liquid (Willeke, Lin & Grinshpun, 2007). The device offers several advantages, including limiting particle bounce and reaerosolization, as well as allowing for more viscous, less evaporative collection liquids than conventional liquid impingers (Willeke, Lin & Grinshpun, 2007).

Willeke, Lin, and Grinshpun (2007) explain the particle bounce phenomenon as when "the force of particle rebounding exceeds the particle adhesion force." They go on to state particle bounce may occur from desiccated collection media as well as other collected particles when samples become overloaded (2007). The swirling motion circulates media to better retain collected particles, thus reducing the incidence of particle bounce occurrences.

The device's second advantage of being able to operate using viscous collection media contributes to reduced reaerosolization (Willeke, Lin & Grinshpun, 2007). Bioaerosol reaerosolization stems from evaporative losses of the collection liquid (Hogan et al., 2005). Less viscous, water-based liquids evaporate readily within liquid impingers as evidenced by the Willeke, Lin, and Grinshpun (2007) study. The authors compared evaporative losses in the Biosampler® relative to the AGI-30 using water as a collection liquid by measuring volume in the devices over time sampled. The results showed a loss of approximately 80 percent of the collection liquid volume over a two-hour sample in the Biosampler® and all the collection liquid volume from the AGI-30 over 90 minutes of sampling. When the authors introduced glycerol as a collection medium, a non-volatile liquid, they observed negligible losses over an eight-hour sampling period. The findings suggest a distinct advantage of using the Biosampler® over the AGI-30 via the use of a

less evaporative collection medium, assuming said media do not negatively affect viability.

The Willeke, Lin & Grinshpun study also evaluated reaerosolization of polystyrene latex spheres (PSL) for the two samplers and demonstrated significantly more reaerosolization for the AGI-30 (2007). Riemenschneider et al. (2010) corroborated this finding. Of note, the Willeke, Lin & Grinshpun study's use of a monodisperse aerosol in PSL could have drawn a stronger conclusion had the authors also used a polydisperse bioaerosol, as naturally generated bioaerosols are very unlikely to be monodisperse.

A later study evaluated reaerosolization of MS2 as a polydisperse bioaerosol using the Biosampler® relative to the AGI-30 (Riemenschneider et al., 2010). The methodology included the preparation of a 20 mL viral suspension within the impingers containing primarily sterile deionized water and 20 µL of phosphate buffer solution (PBS). This detail in this study's method is of consequence as the authors acknowledge the PBS solutes could be aerosolized and erroneously inflate the counts of bioaerosols as condensation particle counters could not differentiate solutes from viral particles. Despite this potential bias, the study produced several consequential conclusions. Firstly, the higher sampler flow rates correlated to higher rates of reaerosolization. Secondly, increasing MS2 concentration in the sampler also contributed to reaerosolization only up to a certain point at which surface tension changes then resulted in a declining reaerosolization rate. Most importantly, the authors found reaerosolization not to play a significant role in lowering collection efficiency (Riemenschneider et al., 2010).

Rather, the study noted the Biosampler's® PSE to be low for the tested mean mode MS2 particle size of 12-81 nm (Riemenschneider et al., 2010). This conclusion echoes one drawn several years earlier by Hogan et al. (2005), who found the PSE of very small particles (10-100 nm) to be below ten percent. The full characterization of the Biosampler's® PSE depicts significant fluctuation based on the aerodynamic diameter of collected particles, a notion substantiated throughout the literature as illustrated in Figure 1.

The advantage of filter-based samplers coupled with sUAS technology is versatility in targeting select particle size ranges with a given filter (Ohms, 2020). Related to this notion, studies have also assessed the PSE of MS2 on gelatin filters against various other filter types (Burton, Grinshpun, & Reponen, 2007). The authors measured the concentration of particles in the 10-80 nm range upstream and downstream of the filter with a wide-range particle spectrometer. The results from this study indicated a PSE greater than 96 percent for the gelatin filters.

A disparate result came from a landmark comparative sampler study using nine different bioaerosol sampling devices with four different bioaerosol types evaluated for both PSE and BSE (Dybwad, Skogan & Blatny, 2014). They found gelatin filters as having approximately 20 percent of the PSE relative to the Biosampler®. The methodology included measuring 4 μm MMAD MS2 containing particles analyzed via quantitative polymerase chain reaction (qPCR). As discussed, the median particle size correlates to collection efficiency. This, along with the different analytical method could partially explain differences in results from the Burton, Grinshpun, and Reponen (2007) study, though these results suggest experimental flaws. The authors characterize the low

MS2 PSE results as a discrepancy, indicated by consistent PSE among all other agents. A supplementary result shows discrepant data points excluded, which then reveal similar PSE of the gelatin filters and the Biosampler® for 4 µm MMAD particles. The authors could have drawn stronger conclusions had they used an additional measurement technique to determine PSE, such as a wide-range particle spectrometer, as with Burton, Grinshpun, and Reponen (2007).

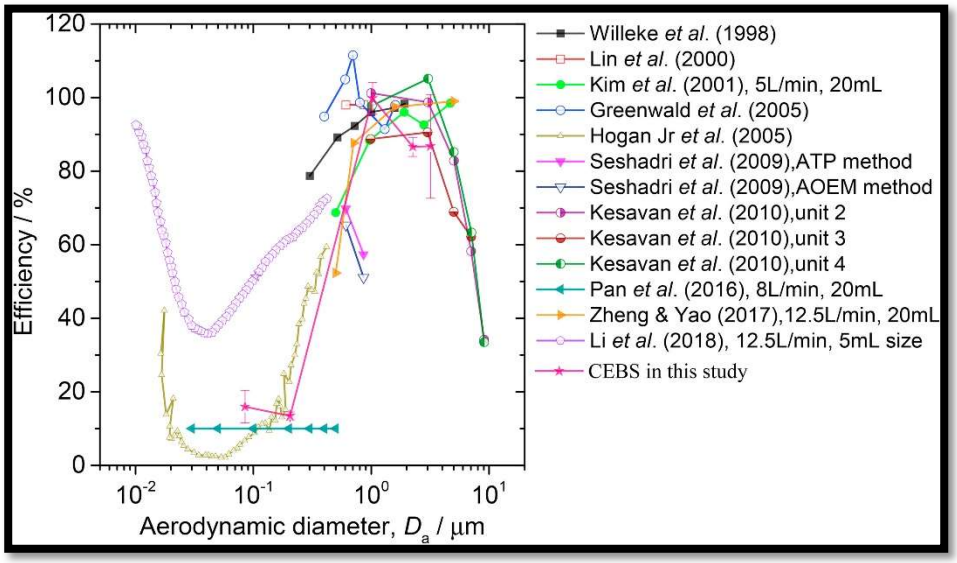

Figure 1. Biosampler® Collection Efficiency by Aerodynamic Diameter in Key Bioaerosol Studies

(From Su et al., 2020. Reprinted with kind permission from Elsevier)

In addition to PSE, sampler preservation of viability may be of higher consequence, depending on the analytical technique and aim of the study. Media desiccation is a notable concern surrounding the use of gelatin filters for bioaerosol studies evaluating viability. Zuo et al. (2014) studied this effect directly by performing a plaque assay in triplicate immediately after the introduction of MS2 and after 15 minutes of HEPA-filtered air had passed over the filter. The results indicated no significant

differences in viability between these conditions. This finding suggests sampling periods less than 15 minutes should not cause desiccation at a level that would significantly bias associated assays for MS2 bacteriophage.

The Dybwad, Skogan, and Blatny (2014) study also evaluated the relative BSE of the Biosampler® and gelatin filters using plaque assays. These results show the gelatin filter slightly exceeded the Biosampler®, suggesting better viability preservation when sampling MS2 (2014). The conclusions of near equivalent BSE for the Biosampler® and gelatin filter are foundational to the design of the study at hand. Moreover, the present study serves to fill a notable weakness in the literature by providing an additional direct BSE comparison of these devices for MS2.

External factors, especially relative humidity, have been shown to influence the sampling efficiencies of bioaerosols. Tseng and Li (2005) evaluated the relative recovery of four different bacteriophages (T7, phi 6, phi x174, and MS2) for four different sampling devices (Anderson impactor, AGI-30, gelatin filters, and nucleopore filters) at three levels of relative humidity (20 percent, 55 percent, and 85 percent). This was a well-designed study that elucidated the effects of humidity by sampler and organism. A key finding relevant to the current study was gelatin filter's relative recovery of MS2 was stable at all three relative humidity levels. This finding supports the field use of the sUAS sampler with gelatin filters for viral collection, understanding that relative humidity levels may fluctuate widely across operational environments. In contrast, Lin, Schenke & Marr (2020) found the relationship between MS2 viability and relative humidity to follow a U-shaped curve, whereby the highest viable concentrations were obtained after exposure to low and high relative humidity (20% and 80%). The lowest viability was

found after exposure to 50% relative humidity conditions. Of note, the study by Lin, Schenke & Marr (2020) pipetted an MS2 suspension onto polystyrene surfaces versus active high-volume air sampling onto gelatin filters, as with Tseng & Li (2005).

Relative humidity also imposes some limitations on the use of the gelatin filters affixed to the sUAS. Relative humidity levels will differently affect the desiccation rates of gelatin media as air moves through and across the filter face. Burton, Grinshpun, and Reponen (2007) observed that this filter type is predisposed to desiccation with longer sampling periods. Low ambient relative humidity will exacerbate this effect. Desiccation of the filters will cause losses in both BSE and PSE to some degree. Thus, low relative humidity environments coupled with extended sampling periods present use limitations for this media type in the collection of viable bioaerosols.

Cooper (2010) points out a general advantage to liquid collection media as eliminating the need for extraction of the bioaerosol sample and transfer between media types which should better preserve viability. This literature review could not ascertain a consensus on the most optimal collection fluid, as media was highly varied by study. Examples of Biosampler® liquid media include sterile DI water (Tseng & Li, 2005), phosphate buffer solutions with (Dybwad, Skogan, and Blatny, 2014) and without (Fabian, McDevitt, Houseman, and Milton, 2009) antifoam chemical additives. Tseng and Li evaluated the effect of three distinct types of collection liquids in the Biosampler® including sterile deionized water, peptone broth, and nutrient broth. The authors cited no discernable difference in resulting viability, though this preliminary data was unpublished (2005). This gap within the literature highlights an important variable for Biosampler®

viral collection study design. Future viability studies should address this question considering the prevalence of the Biosampler's® use within this research space.

Filter-based samplers may pose additional challenges as they often require extraction into liquid media prior to analysis. Extraction of filters is associated with adverse effects on virion viability (Tseng & Li, 2005). Gelatin filters offer a distinct advantage in that they easily dissolve in common liquid media, a property linked to lesser viability losses via extraction (Fabian et al., 2009).

Analytical Methods

A staple viral enumeration technique that quantifies viable viruses is the plaque assay. The double agar layer methodology by Adams (1959) is a governing protocol for phage enumeration (Dubovi Amn & Akers, 1970; Hogan et al., 2005; Tseng & Li, 2005). Adams contends the method "tremendously facilitated the plating of bacterial viruses since it is more rapid than the plating technique" (1959, p.451). In this passage, Adams refers to the pour plate method as having a distinct advantage over the spread plate method. More recent revisions to this method revert to spread plate techniques, citing improved clarity of plaques which enable more precise counts (Cormier & Janes, 2014). In the context of biological agent detection, the rapidity of analysis is a principal consideration. Within this framing, plaque assays of any available type are not rapid as they require overnight incubation to obtain a result (Adams, 1959; Cormier & Janes, 2014). An additional drawback of plaque assay methodology is the underestimation of viral concentration. A study analyzed two types of polioviruses via plaque assay for enumeration (Teunis, Lodder, Heisterkamp, de Roda Husman, 2005). The authors then

typed the viruses in individual plaques via antibody neutralization assays, finding both types of viruses within single plaques. The study demonstrated 1 virion did not correspond to 1 plaque, hence underestimation of viral concentrations may be an inherent bias associated with plaque assays.

A more rapid analytical method vice plaque assays is polymerase chain reaction (PCR), with modern systems typically clocking in at a two-hour analysis time per run (Sakurai et al., 2011). Mullis & Faloona (1987) first described this technology in the literature in the mid-1980s as a means of amplifying nucleic acid sequences (Mullis & Faloona, 1987). PCR analysis enables the qualitative identification of sampled viruses by matching the sample to known sequences of viral DNA or RNA. PCR false positives (or low specificity) were a common challenge in the years following its inception, but have since been mitigated (McCreedy, 1995). High proportions of PCR false negative results have also been demonstrated when paired with the Biosampler® in the collection of MS2 (Cooper, 2010). In this study, confirmation was found through positive results with plaque assays. The author attributed these outcomes to low sample volumes collected by the Biosampler®, thus low viral concentrations that failed to achieve the detection thresholds of the PCR analysis after repeated cycles. Of note, the sUAS used in this study achieved sample volumes of approximately 5 percent relative to those collected by the Biosampler®. Therefore, false negative PCR results may be exacerbated in sUAS-collected viral aerosol samples. There are contrasting conclusions regarding low-concentration samples analyzed by PCR analysis. McCreedy states the sensitivity is high relative to culture-based methods, enabling agent identification in low-concentration samples (1995).

One advantage of the technology is the nature of the analysis does not necessitate the capture of viable organisms in the collected sample. This obviates concerns about sampling-induced stresses, thus allowing a wider selection of viral sampling instrumentation when paired with this analytical method. The tradeoff to using this technique is not ascertaining the infectivity of the agent.

Quantitative PCR is an extension of this analytical technology. However, enumeration for health risk assessment purposes should be secondary to presence/absence determination in an initial biological threat investigation. Moreover, concentration limits governing bioaerosols exposure (indicating levels at which health risks are considered elevated for most exposed individuals) do not exist for several reasons. These include the wide range of human responses, an inadequately described exposure-response relationship, and the fact that bioaerosols comprise many organisms which cannot be deciphered by single samples (ACGIH, 2022). This principle for bioaerosols risk assessments in industrial hygiene contexts may be extended to biological agent responses where agent identification is a leading priority for effective countermeasure initiation.

III. Methodology

Chapter Overview

The purpose of this chapter is to outline sampling and analytical methodologies used within this study. Laboratory methodology includes the preparation of antibiotic, bacterial host, and bacteriophage stocks. Additionally, the enumeration process of the phage stock is described, with procedures also applying to sample analysis. Following this, aerosolization and sampling procedures are explained, including the retrieval and storage of samples prior to analysis. Finally, the plaque assay process for a given sample day is defined, including control plating. All research was conducted under institutional biosafety committee protocol IBCR#2020-02-26-001-COOPERC and ALFI 20-01.

Initial Laboratory Preparation – Phage, Host, and Antibiotic Stocks

MS2 bacteriophage was chosen as a model viral organism for this study. The specific phage used was American Type Culture Collection (ATCC) 15597-B1, Escherichia coli bacteriophage MS2 (Manassas, VA). Prior to phage propagation, it was first necessary to prepare antibiotic stock as well as the host bacteria stock (ATCC 15597, Escherichia coli (Migula) Castellani and Chalmers, Manassas, VA).

Antibiotic Stock Preparation

The addition of select antibiotics in the host bacteria culture necessitates antibiotic resistance among the bacterial cells via F-factor plasmids. These plasmids code for pili formation (EPA, 2018). According to the EPA, these filamentous structures on the exterior of the *E. coli* cell serve as a means for *E. coli* to transfer nucleic acid between cells (2018). In effect, the bacterial cells use these structures to communicate

intercellularly. Additionally, pili are the site of attachment and infection for MS2 bacteriophage (EPA, 2018). An image of this attachment process captured via transmission electron microscope (TEM) is depicted in Figure 2.

Antibiotics were prepared in accordance with EPA Method 1643 (2018). Preparation was conducted under a Class II Biological Safety Cabinet (BSC) (Baker Company, Sanford, ME) to ensure product protection from external contaminants. The antibiotic solution consisted of streptomycin sulfate (Sigma-Aldrich, S6501, St. Louis, MO) and ampicillin sodium salt (Sigma-Aldrich, A9518, St. Louis, MO). Antibiotic quantities of 0.15 g ampicillin and 0.15 g streptomycin were dissolved per 100 mL of cooled sterile deionized water in a shaker flask via hand swirling. Once dissolved, the antibiotic solution (amp/strep) was aseptically filtered through a 0.22 µm pore size syringe filter (Fisher Scientific, Waltham, MA) into 15 mL conical tubes. The tubes were then sealed and wrapped in aluminum foil for extended freezer storage at -20 degrees Celsius (°C), consistent with manufacturer guidance (Sigma-Aldrich, 2022).

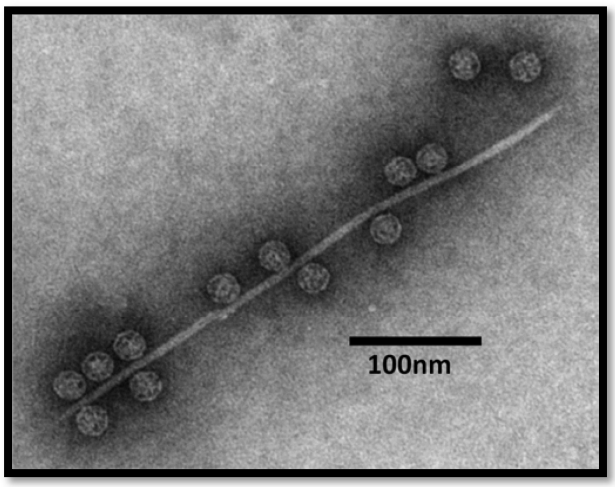

Figure 2. TEM Image of MS2 Bacteriophage on E.coli Pilus

(From Wong et al., 2014. Reprinted with kind permission from Elsevier)

E. coli Glycerol Stock Preparation

E. coli stocks were prepared following the EPA Method 1643 with slight deviations in culturing technique. Freeze-dried host bacteria were rehydrated and cultured in trypticase soy broth (TSB) (Becton, Dickinson and Company, Sparks, MD). TSB consisted of 17 g pancreatic digest of casein, 3 g papaic digest of soybean, 2.5 g dextrose, 5 g sodium chloride, and 2.5 g dipotassium phosphate. TSB was prepared at a concentration of 30 g per 1000 mL of deionized water. To accomplish this, TSB was weighed using a microbalance (Sartorius, Goettingen, Germany). Weighed TSB was slowly added into a glass screw-top bottle by hand swirling until dissolved. The solution was then loosely capped and autoclaved at 121°C and 15 pounds per square inch (psi) for 30 minutes. After cooling to under 48°C, antibiotics were added at volumes of 10 mL amp/strep to 1000 mL TSB. The solution was then hand swirled for approximately 30 seconds. Next, 1 mL of the freeze-dried host was added aseptically to 25 mL of TSB in a 50 mL conical tube. An initial overnight culture of 18 hours was performed, followed by a log phase culture of 4 hours. The log phase culture required 1 mL of the overnight culture added to 25 mL sterile and cooled TSB. Both broth cultures were incubated in a VWR CO_2 incubator (Radnor, PA) at approximately 36°C.

Next, ultrapure glycerol (Alfa Aesar, Ward Hill, MA) was autoclaved at 121°C and 15 psi for 30 minutes. After cooling to under 48°C, the sterile glycerol was combined with the log phase *E. coli* culture at a ratio of 1:4, with glycerol being the lesser component. The mixture was hand swirled in a shaker flask. Following this, 1 mL of the solution was aseptically transferred into 1.5 mL microcentrifuge tubes for extended storage at -80°C.

Phage Stock Preparation and Titer

The first step to phage propagation was to prepare a log phase host culture. Sterile TSB was prepared by dissolving 30 g TSB per 1000 mL deionized water and then autoclaving for 30 minutes at 121°C and 15 psi. Once cooled to under 48°C, 1 mL of the frozen stock was thawed to a liquid state then aseptically transferred into a 50 mL conical centrifuge tube along with 25 mL of sterile TSB with amp/strep. After hand swirling, the culture was incubated for 18 hours at approximately 36°C. The following day, 1 mL of the overnight culture was added to 25 mL sterile, cooled TSB with amp/strep in a second 50 mL conical centrifuge tube. The culture was hand swirled and incubated for another 4 hours at 36°C to achieve log phase.

Thereafter, 1 mL of the freeze-dried phage was added to the 25 mL log phase host culture. The mixture was hand swirled and incubated at approximately 36°C for 24 hours. The phage/host mixture was then centrifuged at 3500 rotations per minute (rpm) for 10 minutes to separate heavier *E. coli* cells and debris from phages. Following this, under a BSC, the supernatant was filtered through a 22 µm membrane filter into an amber glass screw-top vessel. The vessel was capped and sealed with Parafilm®, wrapped in aluminum foil to prevent any UV or visible light inactivation of the phage, then stored at 4°C. These storage conditions were found to best limit the decay of MS2 for a period under 40 days (Olson, Axler & Hicks, 2004).

Plaque Assay Process

Titers were accomplished before, at the midpoint, and immediately following experimental trials. The purpose of this enumeration was to ensure aerosolized

concentrations did not significantly differ due to the natural decay of the bacteriophage. Titers were accomplished using a derivation of the Adams (1959) double agar layer plaque assay method. Post-sampling plaque assay analysis was also accomplished using this methodology, only differing by serial dilutions used.

Bottom Layer Plate Preparation

All plating within this study was conducted under a Class II BSC. The plates utilized in this study were Fisherbrand™ (Fisher Scientific, Waltham, MA) 100 mm disposable Petri dishes. The 1.5% Trypticase Soy Agar (TSA) bottom layer of the double agar layer consists of solidified agar and TSB with added amp/strep. The inert ingredients serve as a growth medium for host bacteria, thus allowing for subsequent infection by the MS2 bacteriophage.

Sample plates were first labeled with sample number, corresponding sampling device, date of plate preparation, and serial dilution. Control plates were labeled similarly. The plates were made by weighing 30 g TSB and 15 g agar per 1000 mL of deionized water. The weighed ingredients were then slowly added into glass screw-top jars via hand swirling until dissolved. The jars were loosely capped and autoclaved at 121°C and 15 psi for 30 minutes. The molten 1.5% TSA was allowed to cool to less than 50°C, at which point thawed antibiotic stocks could be added. 10 mL of antibiotic stock were added per 1000 mL of 1.5% TSA and mixed by hand swirling. Consistent with EPA method 1643, 17-18 mL of 1.5% TSA with amp/strep were pipetted into plate bottoms. After approximately 10 minutes of cooling until solidified, plates were capped and inverted to prevent condensation from forming on the media surface. All plates were

prepared ahead of experimentation and stored at 4°C for no longer than 1 week and wrapped in polyethylene and aluminum foil.

Serial Dilutions

Serial dilutions were accomplished to dilute the starting phage stock solution to known dilution increments. This process allows for more accurate enumeration as the volume of the undiluted sample represents the mL variable in the PFU/mL concentration equation. This will be described in further detail in the *Plaque Counting and Enumeration* section. Dilutions were performed several hours prior to the top agar overlay to prevent phage decay from extended storage. 1.5 mL microcentrifuge tubes were labeled in descending dilutions (e.g., 10^{-1} through 10^{-11}).

Sterile deionized water was used as the diluent. Dilutions began with the least diluted 10^{-1} tube where 900 µL of sterile deionized water and 100 µL of phage stock solution were micro-pipetted into the respective tube. The contents were vortexed using the A. Daigger & Co. Vortex Genie 2 (Hamilton, NJ) for 5 seconds before progressing to the next dilution. The 10^{-2} tube was inoculated with 900 µL of sterile deionized water and 100 µL of the 10^{-1} tube. This sequence progressed similarly to the desired dilution. The serial dilution process is illustrated in Figure 3.

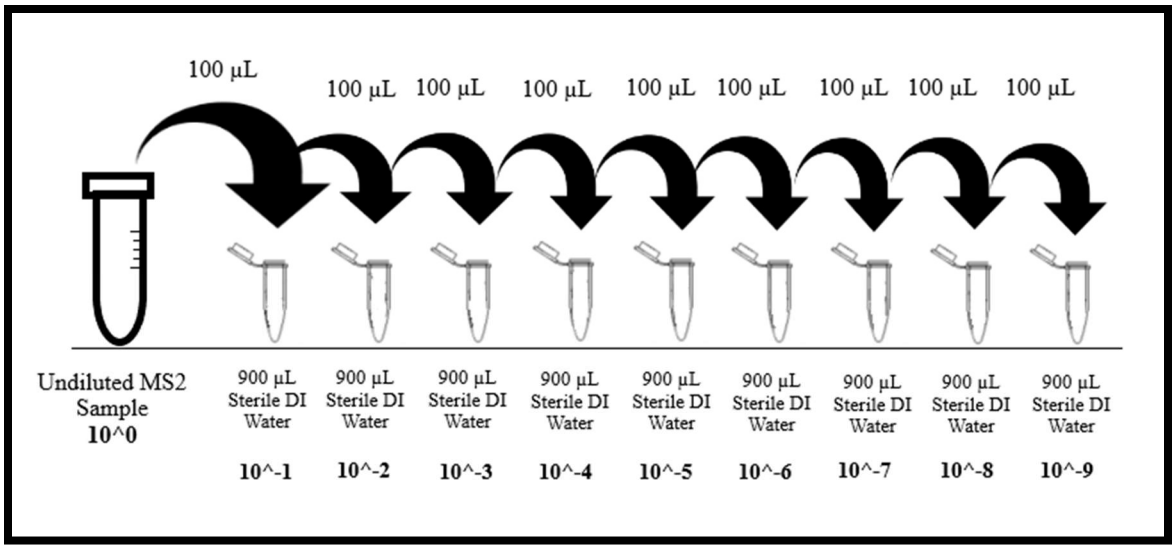

Figure 3. Serial Dilution Process

Top Layer Agar Overlay Preparation

A log phase host culture was needed prior to the top layer agar process. As previously described, this required an 18-hour incubation of 25 mL TSB with amp/strep and 1 mL *E. coli* stock followed by a 4-hour incubation of a second vial of 25 mL TSB with amp/strep and 1 mL of the overnight culture, both at approximately 36°C. If the incubation of the log phase culture did not align with the cooling of the molten top agar, the host culture was stored at 4°C until use to prevent host overgrowth.

Bottom layer plates were removed from refrigerated storage and brought to room temperature within the BSC. The top layer 0.7% TSA was prepared with the same ingredients as the bottom layer, but with reduced agar concentration (30 g TSB and 7 g agar per 1000 mL DI water). Ingredients were weighed and added to the solution in a glass screw-top jar. Dissolution was achieved by hand swirling. Next, the 0.7% TSA was autoclaved at 121°C and 15 psi for 30 minutes. The molten TSA was allowed to cool to under 50°C, at which point antibiotic stock was added at a concentration of 10 mL

amp/strep per 1000 mL TSA. The customary warm bath was not used to keep agar molten due to limited space within the BSC and concerns of cross-contamination. Instead, 3-4 vessels containing approximately 300 mL of 0.7% TSA were removed from the autoclave at chronological intervals. This ensured agar temperatures maintained a molten state throughout the top agar overlay process with considerations to avoid scorching of the media.

Top Agar Layer Overlay Process

Sterile 15 mL glass test tubes were used as a mixing and transfer vessel for the overlay process. The process was initiated when the TSA was measured at a temperature of 49°C or cooler, as temperatures exceeding this lead to rapid inactivation of the *E. coli* host. The overlay process was accomplished in sequences of 3 overlays in short succession. The 3 overlays ensured inoculation and pouring corresponded to the appropriate triplicate samples. The short sequences also ensured the agar remained in a molten state.

First, the 3 serial dilutions to be plated were vortexed for 5 seconds to homogenize each sample. Next, 5 mL of 0.7% TSA was dispensed into 3 test tubes. 500 µL of the serial dilution was inoculated into the molten agar followed immediately by the inoculation of 100 µL of *E. coli*. The tubes were tilted slightly off vertical between gloved hands and rolled to mix the contents for several seconds. The tube contents were then poured to the corresponding plate. The plates were tilted from the horizontal position in a figure-8 pattern to evenly distribute the molten top agar across the entire bottom layer surface. The plates were allowed to cool for approximately 10 minutes, after which they were capped, inverted, and incubated at 36°C for 16-24 hours.

Plaque Counting and Enumeration

Plaques are circular areas that clearly contrast from the otherwise milky bacterial host lawn (Marintcheva, 2018). According to Marintcheva (2018), plaques are formed as a consequence of a single virus lysing a bacterial cell as newly made virions are released into the surrounding milieu. Plaque countable ranges represent bounds within which counts may be used to determine the PFU/mL concentration. This study employed a countable range of 1-200 plaques. Plaque ranges within the literature vary with the upper bound as high as 300 plaques (EPA). A pilot study informed the reduction of the upper bound to 200 plaques, as higher counts resulted in substantial plaque overlap, hence a higher likelihood of inaccurate counts. Counts outside of the upper bound were identified as too numerous to count (TNTC) and left out of enumeration equations. Similarly, non-detect plates with 0 plaques were excluded. All plaque counts were accomplished manually by identifying all plaques with a small written mark. Lastly, the total count was written on each plate. Counted plates are depicted in Figure 4. The enumeration calculation is shown in Equation 1 (adapted from EPA, 2018).

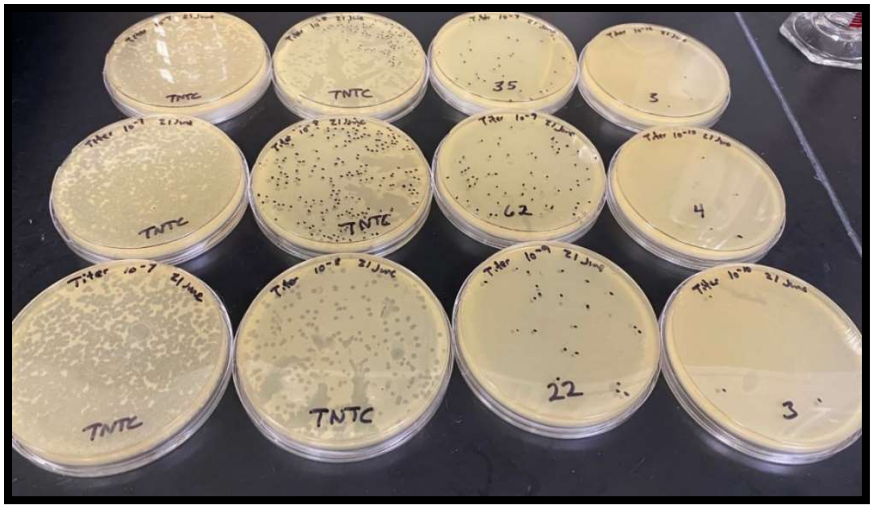

Figure 4. Plates with Counted Plaques

$$Undiluted\ Phage\ Concentration\ \left(\frac{PFU}{mL}\right) = \frac{PFU_1 + PFU_2 + \ldots PFU_n}{V_1 + V_2 + \ldots V_n} \quad (1)$$

Where

PFU = Number of counted plaques within countable range (1-200)

V = Volume in mL of undiluted sample

n = Representing any additional plates containing plaques within countable range and corresponding undiluted sample volume

MURPHEE Chamber Setup

All MS2 aerosolization and sampling were conducted within the MURPHEE chamber. The chamber was measured at 0.914 m × 0.914 m × 6.401 m (3 ft × 3 ft ×21 ft) and is depicted in Figure 5 (Chapman, 2021). The MURPHEE air velocity, as previously characterized, was 0.2 meters per second (m/s), corresponding to the centrifugal fan (fan manufacturer) setting of 16 Hertz (Ohms, 2020; Harvey, 2022; Fuller, 2022). The fan pulled air through a high-efficiency particulate air (HEPA) filter at the inlet of the chamber and again through a HEPA filter at the chamber outlet, nearest the fan.

Prior to experimentation, the fan was turned on and all internal surfaces of the MURPHEE chamber, clamp stands, polyethylene connecting tubing, and sUAS mount and components were sprayed or wiped with Clorox Fuzion® disinfectant. The disinfectant was allowed to contact for at least 15 minutes, followed by wiping any surfaces to which it was applied with DI water to remove any inert residue. The selected disinfectant is self-neutralizing, meaning it will not leave corrosive or reactive residues on experimental components and equipment (Cooper, Aithinne, Stevenson, Black & Johnson, 2020).

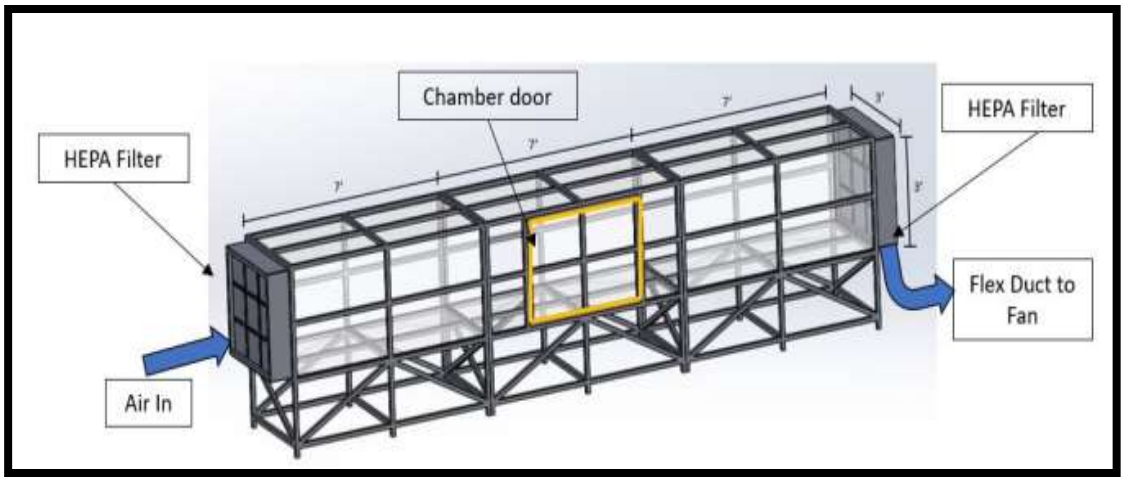

Figure 5. MURPHEE Aerosol Chamber (Chapman, 2021)

After disinfection, equipment was arranged within the chamber beginning with the Collison nebulizer furthest upstream of the fan. Continuing further downstream towards the fan inlet, the sUAS was then placed followed by the Biosampler®. The Collison nebulizer and Biosampler® were elevated using clamp stands, while the sUAS sampler was elevated via the hover mount developed by Fuller (2022) and Harvey (2022). The narrow width of the chamber precluded sampling devices from being side-by-side. The experimental arrangement and respective measurements are depicted in Figure 6.

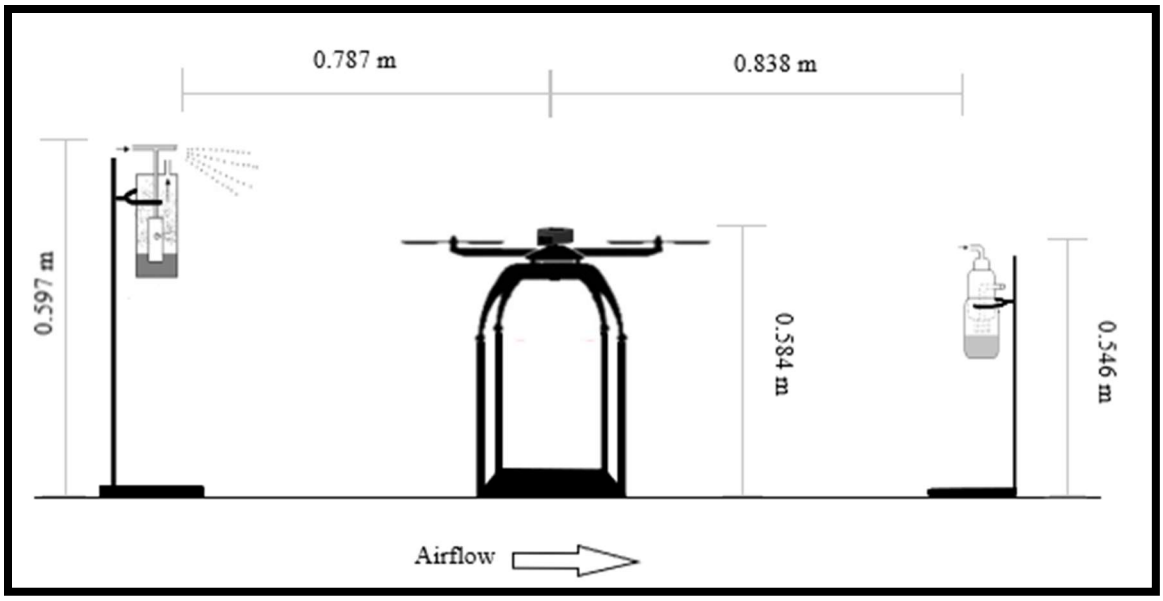

Figure 6. MURPHEE Chamber Experimental Setup (not to scale)

Collison Nebulizer Setup

The 6-jet Collison nebulizer (CH Technologies, Westwood, NJ) was prepared using the MS2 bacteriophage stock solution diluted with sterile deionized water at a 1:10 ratio. The total liquid volume of the Collison is recommended by the manufacturer at 40 mL; thus, 4 mL phage stock (vortexed for 5 seconds) and 36 mL sterile DI water were added to the sterile reservoir, then hand swirled. The sterile nozzle cap was screwed in place and then clamped onto the clamp stand at the premeasured height shown in Figure 6. Flexible polyethylene tubing was used to deliver pressurized air inflow to the Collison nebulizer inlet through drilled port holes in the MURPHEE chamber. A HEPA filter was used in-line so as to not introduce contamination into the MURPHEE. Gaps between holes and tubing were sealed with duct tape. Electrical tape was used to further secure tubing to Collison inlet to prevent detachment during trials. The Collison inflow was measured using an Alicat Scientific mass flow meter (M-Series, Tucson, AZ) with an

average flow rate of 7.5 liters per minute (lpm) and 14.24 psi. This pressure inflow corresponds to the measured particle size distribution as shown in Figure 7. Particles sizes fell within 1 of 6 bins ranging from 0.3 µm – 10 µm. Measurements were obtained with a Particles Plus Particle Counter, Model 8306 (Stoughton, MA). A one minute sample was collected after 20 minutes of aerosolization. Background measurements were subtracted from final counts. Full results may be found in Appendix J.

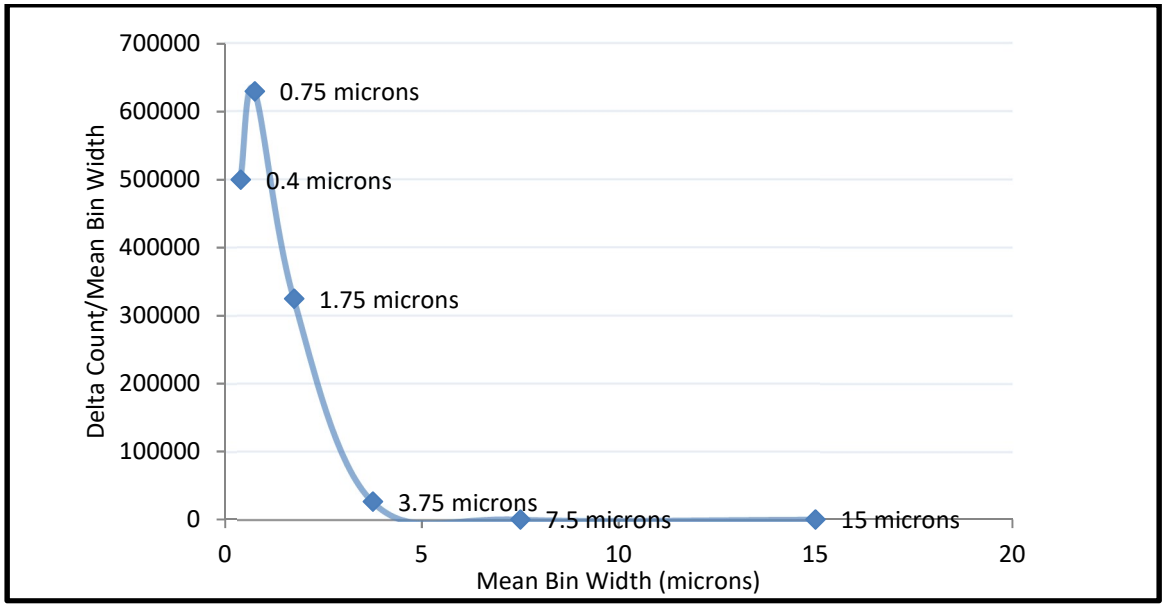

Figure 7. Collison Nebulizer-Generated MS2 Aerosol Particle Size Distribution

Biosampler® Setup

Calibration of the Biosampler® was performed before and after trials on each day of sampling using the Mesa Labs Bios Drycal Defender 510 (Lakewood, CO). A burst setting of 10 sequential calibration measurements was completed and the average flow rate was recorded. In-trial flow rate verification was also accomplished via a precision rotameter.

The Biosampler® has a manufacturer-suggested liquid collection media volume of 20 mL and a flow rate of 12.5 lpm. Adjustment of these parameters for viral aerosols has demonstrated increases in viable recoveries (Zheng & Yao, 2017). This study deviated slightly from the suggested airflow rate, selecting 12 lpm, based on previous studies supporting a lower flow rate for MS2 aerosol collection (Turgeon, Toulouse, Martel, Moineau & Duchaine, 2014; Anwar, Oh & Wu, 2010). PBS was selected as the liquid collection media based on pilot data indicating better preservation of viability relative to sterile deionized water as a medium.

First, 20 mL of 1x PBS (Sigma-Aldrich, P5493, St. Louis, MO) were added aseptically to the sterile reservoir. The device was then assembled and attached to the clamp stand at the premeasured height. A flexible polyethylene tube was connected to the Biosampler® outlet, threaded externally through a drilled porthole in the side of the chamber, connected to an in-line HEPA filter, then affixed to the high-volume sampling pump (SKC Biolite, Model 228-9615, S/N 20549645, Eighty-Four, PA).

sUAS Setup

Calibration of the sUAS sampler was performed before and after trials on each sampling day, accomplished using the TSI Inc. 4100 Series flow-through meter (Shoreview, MN). Three measurements were taken, then the average was recorded, consistent with OSHA Technical Manual calibration guidance (2014). The average across all trials was approximately 0.63 lpm. An image of this calibration setup is shown in Figure 8.

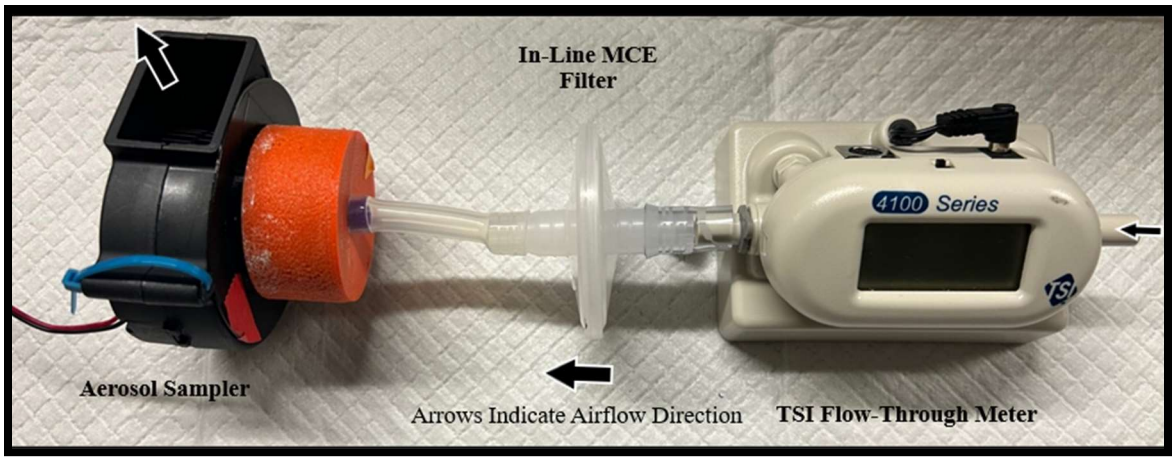

Figure 8. sUAS Sampler Calibration Train

sUAS setup began by attaching power and servo driver cords to the power source and remote control. As with the other equipment, all cords were threaded through drilled ports in the chamber wall. A lead brick was placed at the base of the mount to ensure the sUAS would remain in a fixed position when its rotors were in operation. The filter-based sampler, designed by Ohms (2020), consisted of a 12V Brushless Fan (Fugetek, Houston, TX) and a 3D-printed filter mount, held in place by bolts and wingnuts on either side. The fan power cords were similarly threaded externally through the MURPHEE chamber. This device attached to the sUAS in sampling configuration is shown in Figure 9.

The selected SKC gelatin filters were 37 mm in diameter, 250 µm thick, with an approximate pore size of 3 µm (Cat No. 225-9552, Lot 112012602200180, Eighty-Four, PA). Filters were stored at 4°C until immediately prior to use. Sterile forceps were used to insert the filter into the mount. The mount was secured to the sampler by hand-tightening wingnuts onto both bolts. The sampler was then attached to the top of the sUAS via hook-and-loop strips. The positioning of the sampler on the top of the sUAS was based on findings of more consistent results versus attachment underneath the sUAS

body (Ohms, 2020). The sampler power cord connectors were attached, and MURPHEE chamber access door was closed and sealed with duct tape.

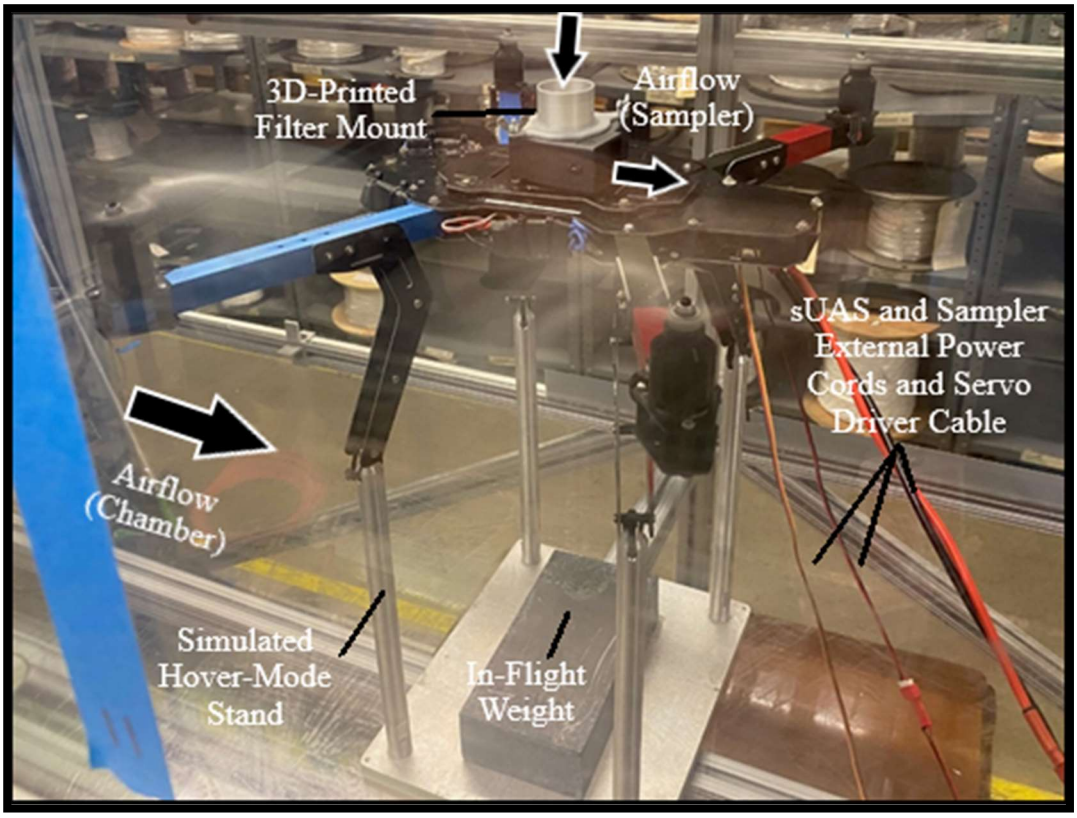

Figure 9. sUAS with Attached Sampler

Sampling Procedure

In total, 10 controls and 30 samples were collected for both devices across 10 days of sampling. Sampling days consisted of 1 control trial followed by 3 sampling trials. The control trial was to ensure the MURPHEE chamber and sampling equipment were free of bioaerosol contamination which may have interfered with the results. Control trials differed only by the omission of MS2 aerosolization. All other procedures are described below for the sampling process.

The Collison nebulizer air pressure in-flow was initiated for MS2 aerosolization. Simultaneously, the sUAS rotors were turned via the servo driver at a setting of 1400 microseconds (μs). The rotors were run as an ad hoc means of air mixing throughout experimentation. The chamber was allowed to equilibrate for 5 minutes. Ambient pressure, MURPHEE chamber temperature, and chamber relative humidity were recorded.

At the end of this period, the Biosampler® and sUAS sampler were simultaneously initiated for a 15-minute sample collection. Rotor speeds were maintained at 1400 μs (equivalent to 40% power on a linear curve), meant to simulate the hovering of the device while collecting a sample (Fuller, 2022). After the sampling period was completed, all equipment was turned off, including the Collison nebulizer air flow, sUAS rotors and sampler, and Biosampler®. The MURPHEE chamber remained sealed for 5 minutes to purge suspended MS2 via chamber airflow and filtration. The 5-minute purge time was precedent from Fuller (2022) and Harvey (2022), who noted no residual contamination between successive trials using this method.

First, the sUAS filter was detached to retrieve the gelatin filter media, as it was prone to desiccation with prolonged exposure to ambient conditions. Sterile forceps were used to place the filter into a 50 mL conical tube containing 20 mL of PBS. The filters were hand swirled until dissolved based on a study by Dybwad, Skogan, and Blatny (2014). The dissolution of the filters took approximately 30-60 seconds. The conical tubes were then sealed with Parafilm®, placed in a biological material transport bag, and stored at 4°C until analysis.

Next, the Biosampler® was retrieved from the MURPHEE chamber. The collection media contents were hand swirled within the device for 5 seconds before pouring into a 50 mL conical tube. The volume of Biosampler® liquid remaining after sampling was recorded using the increments on the conical tube itself. The tube was then sealed and stored as described for the sUAS sample.

As 3 sampling trials with aerosolization occurred in succession on sampling days, the volume of Collison liquid would decrease slightly over time. Between trials, the Collison nebulizer was checked for nozzle inlet depth of approximately 1 cm to ensure a steady aerosol stream for each trial. The average volume lost per trial was approximately 7-8 mL.

Decontamination

All MURPHEE surfaces, sUAS mount, body, and rotors were sprayed or wiped with Clorox Fuzion® disinfectant and allowed at least 15 minutes of contact time. DI water was then used with wipes to remove any residue from the disinfectant. Collison nebulizer and Biosampler® components were disassembled, rinsed with DI water, and wrapped in aluminum foil. Following this, parts were autoclaved at 121°C and 15 psi for 30 minutes. Filter mounts were decontaminated by submersion in a 10% bleach solution, followed by submersion in sterile deionized water, each for 15 minutes.

Laboratory Analysis

Samples were transported at 4°C from the research facility to AFIT laboratories for analysis. Analysis of samples was accomplished as previously described in the *Plaque*

Assay Process section. A depiction of the overlay process of the top agar layer is shown in Figure 10.

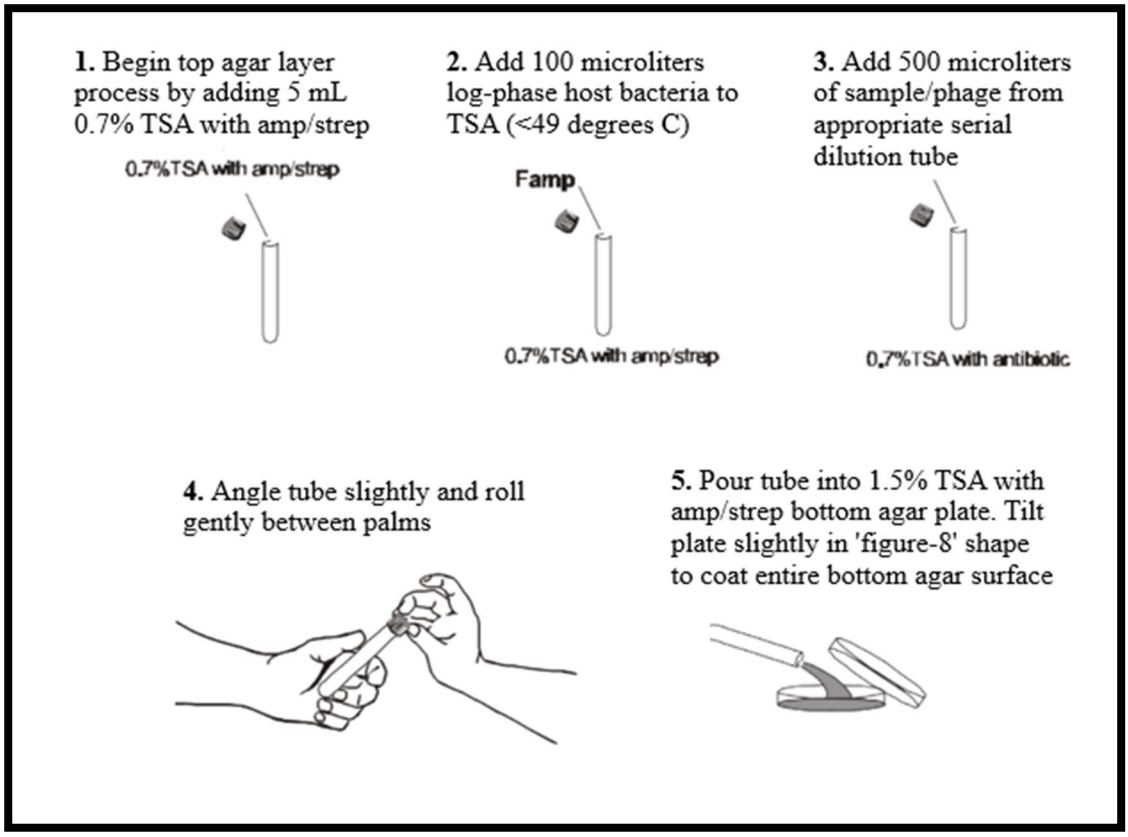

Figure 10. Double Agar Overlay Process (Adapted from EPA, 2001).

For a single day of sampling, 54 plates were used for sample analysis along with 18 control plates for a total of 72 plates. A description of plate types and quantities for samples and controls are shown in Table 1 and Table 2, respectively.

Controls consisted of both sampling and analytical controls. For the sUAS and Biosampler® sample controls, plating differed from other types slightly in that no vortexing of the media was accomplished to prevent inactivating any potential bacterial contaminants. Negative growth on these controls affirmed decontamination procedures were effective. Media control plates were performed using only top and bottom layer

TSA with no host or phage inoculum. Negative growth on these plates affirmed laboratory practice and BSC did not introduce cross-contamination. *E. coli* positive control plates were made using the pour plate method without the phage inoculum. Their purpose was to ensure the host bacteria was active in all plates as indicated by the formation of an opaque lawn. MS2 positive spot plates were prepared by adding only host inoculum to the molten agar in the 15 mL tube. The tube was then poured, contents evenly dispersed across the bottom layer agar, and allowed to solidify for several minutes. Next, a small random inoculum of the phage was dispensed onto the hardened agar. Post incubation, these plates have large tracts free of agar indicating the viability of MS2 stock, the presence of infectable male *E. coli* hosts, and a suitable environment supporting viral propagation. Lastly, MS2 aerosolization media taken from the Collison nebulizer after sampling was also analyzed undiluted to ensure the virus remained in a viable state after aerosolization, transport, and storage prior to analysis.

Table 1. Sample Plates (For 1 Day of Sampling)

Identifier	Device	Plate Type	Number of Plates
Sample Trial 1	Biosampler	10^{-1}	3
		10^{-2}	3
		10^{-3}	3
	sUAS	10^{-1}	3
		10^{-2}	3
		10^{-3}	3
Sample Trial 2	Biosampler	10^{-1}	3
		10^{-2}	3
		10^{-3}	3
	sUAS	10^{-1}	3
		10^{-2}	3
		10^{-3}	3
Sample Trial 3	Biosampler	10^{-1}	3
		10^{-2}	3
		10^{-3}	3
	sUAS	10^{-1}	3
		10^{-2}	3
		10^{-3}	3
Total			54

Table 2. Control Plates (For 1 Day of Sampling)

Identifier	Device	Plate Type	Number of Plates
Sample Control	Biosampler	Growth - 10^0 (Negative)	3
	sUAS	Growth - 10^0 (Negative)	3
Lab Control	N/A	Media Growth (Negative)	3
		E.coli (Positive)	3
		MS2 Spot (Positive)	3
Aerosolization Media (Post Sampling)	Collison Nebulizer	10^0	3
Total			18

IV. Analysis and Results

Chapter Overview

This chapter includes the conversion of raw laboratory analytical results in PFU/mL of sampling liquid to the comparable PFU/L of air sampled. Additionally, the correction of air volumes by recorded temperatures and pressures is presented. Distributions of PFU/L for each device are evaluated along with potential outlier identification. Next, relative BSEs are calculated by trial to be used for a mean relative BSE and 95% confidence interval. Following this, a test of the means is performed using the Wilcoxon Signed-Rank test. Finally, sources of uncertainty are presented. Statistical analysis was performed using JMP® Pro version 15.0.0.

Phage Stock Titer Results

Phage stock was enumerated before, during, and after trials to ensure analogous concentrations were aerosolized throughout experimentation. Results of these titers showed variability, though the slight changes in aerosolized concentration are not expected to impact relative BSE as the same phage solution was used for each device by trial. Full results of the titers and approximate aerosolization concentrations may be found in Appendix G, Table G1.

Experimental Plaque Assay Raw Results

Plaque assays yielded results in PFU/mL as described in Equation 1. These units do not allow the direct comparison of the Biosampler® and sUAS to obtain a relative BSE. They do, however, illustrate a difference in total viable virions collected per device when the liquid matrix volume in which the samples were collected or dissolved is used

to calculate total PFU. This calculation is depicted in Equation 2. This equation accounted for differences in total sample liquid volumes for the Biosampler® trials. These variations were a consequence of evaporative losses throughout a given sampling period. A standard 20 mL of PBS was used for the dissolution of retrieved gelatin filters. Thus, this volume was used to isolate the total PFU for sUAS-mounted gelatin filter samples. These variables and plaque assay concentrations from the 30 experimental trials are shown in Appendix A, Tables A1, and A2.

$$PFU = \frac{PFU}{mL} \times mL \tag{2}$$

Where

PFU = Total plaque forming units collected in a trial

PFU/mL = Plaque assay result accounting for inoculum volume of the undiluted sample

mL = Volume of the liquid sample matrix

Of note, trials 25-27 yielded no plaques for both devices. These anomalous data points were most likely caused by contamination or spoilage of the PBS liquid sampling media within which virions were captured and/or stored until analysis. This conclusion is supported by control plate indications. Pictured in Figure 11, controls show active *E. coli*, MS2 stock, and negative indications of bacterial interferents from the chamber or media. Most notably, viable virions resulting in TNTC plaques are present on plates of the post-aerosolization Collison nebulizer fluid. Only the samples that used PBS media produced no MS2 plaques. Thus, trials 25-27 were excluded from statistical analyses. Subsequent trials were performed using newly made PBS and no further viability issues arose. Full plaque assay results in PFU/mL concentrations may be found in Appendix A.

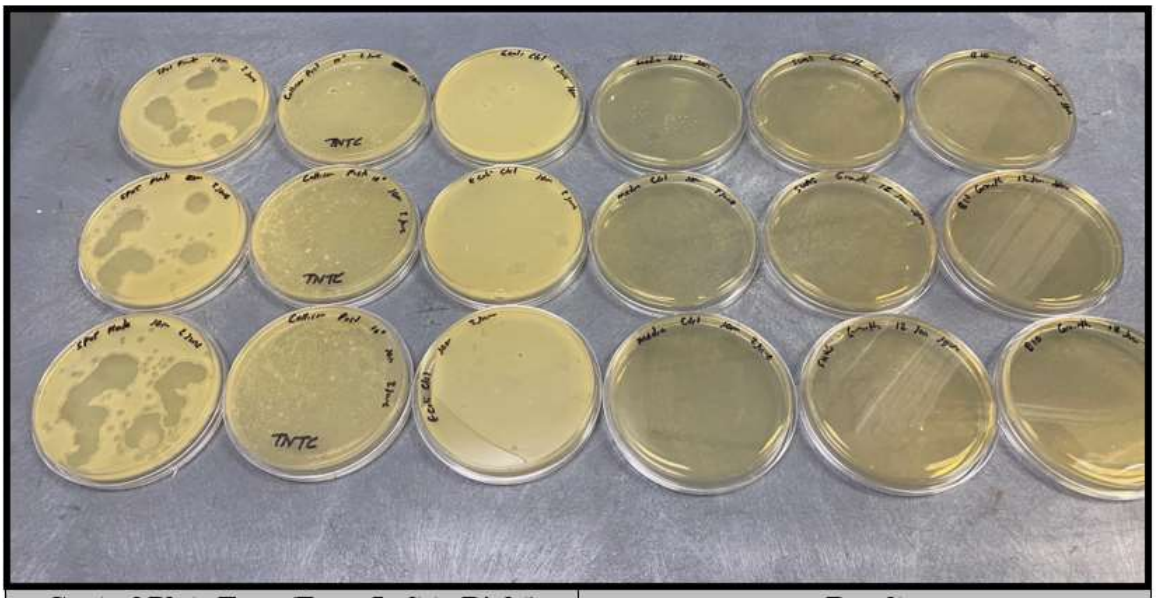

Control Plate Type (From Left to Right)	Result
MS2 Spot Plate	Positive
Collison Nebulizer 10^0 Post Trial	Too Numerous to Count
E. coli	Positive
Media	Negative
sUAS Control Trial Growth	Negative
Biosampler® Control Trial Growth	Negative

Figure 11. Trials 25-27 Control Plates

Air Concentration Results

Next, raw results from plaque assays were converted to total PFU per volume of air collected (L). Volumes were obtained using flow rates and sampling times, then corrected to ambient temperature, and pressure. Average flow rates using the pre- and post-trial calibration were selected for this calculation. The validity of the sample was confirmed by ensuring the flow rates did not differ by more than 5 percent as shown in Equations 3 and 4 (OSHA, 2014). No calibration measurements exceeded this difference as shown in Appendix B, Table B1.

$$Flow\ Rate\ Difference\ (lpm) = \quad (3)$$

$$Pre\ calibration\ Flow\ Rate\ - Post\ calibration\ Flow\ Rate$$

$$Flow\ Rate\ Difference\ (\%) = \frac{Flow\ Rate\ Difference\ (lpm)}{Pre\ calibration\ Flow\ Rate} \quad (4)$$

Where

Pre-calibration flow rate = Primary standard Avg of 3 or 10 measurements, depending on the device (in lpm)

Post-calibration flow rate = Primary standard Avg of 3 or 10 measurements, depending on the device (in lpm)

Next, sample volumes were calculated using average flow rates multiplied by the standardized sampling time of 15 minutes, as depicted in Equation 5.

$$Sample\ Volume\ (L) = Sampling\ Time\ \times Flow\ Rate \quad (5)$$

Where

Sample Volume = Liters of air drawn through sampling pump/media

Sampling Time = Minutes elapsed while pumps were in operation

Flow Rate = lpm as determined by the average of pre- and post-calibration measurements

Sample volumes determined from Equation 5 were then corrected for measured in-chamber temperature and ambient pressure. The calculation for this correction is shown in Equation 6. Full results of the corrected sample volumes are available in Appendix C, Table C1.

$$Corrected\ Sample\ Volume\ (L) = Sampling\ Volume \times \frac{Ambient\ Pressure}{Standard\ Pressure} \times \frac{Standard\ Temperature}{Chamber\ Temperature} \quad (6)$$

Where

Sampling Volume = Uncorrected liters of air drawn through sampling pump/media

Ambient Pressure = Air Pressure Atmospheres (atm)

Standard Pressure = 1 atm

Standard Temperature = Absolute temperature of 298°K

Chamber Temperature = Recorded temperature within MURPHEE in °K

Lastly, sample concentrations in PFU/L were calculated using total PFU over corrected air volumes. Air concentration results by trial for both devices are shown in Figure 12.

Distributions of concentration data from each device in PFU/L were assessed for normality using the Anderson-Darling goodness-of-fit test shown in Figures 13 and 14. Full results are depicted in Appendix E, Figures E1, and E2. The green line represents the normal distribution goodness-of-fit, while the blue line represents a lognormal goodness-of-fit. The results of these tests produced a significant p-value of less than 0.05, prompting a rejection of the null hypothesis of a normal distribution. A lognormal fit was also attempted. These tests showed a failure to reject a lognormal distribution.

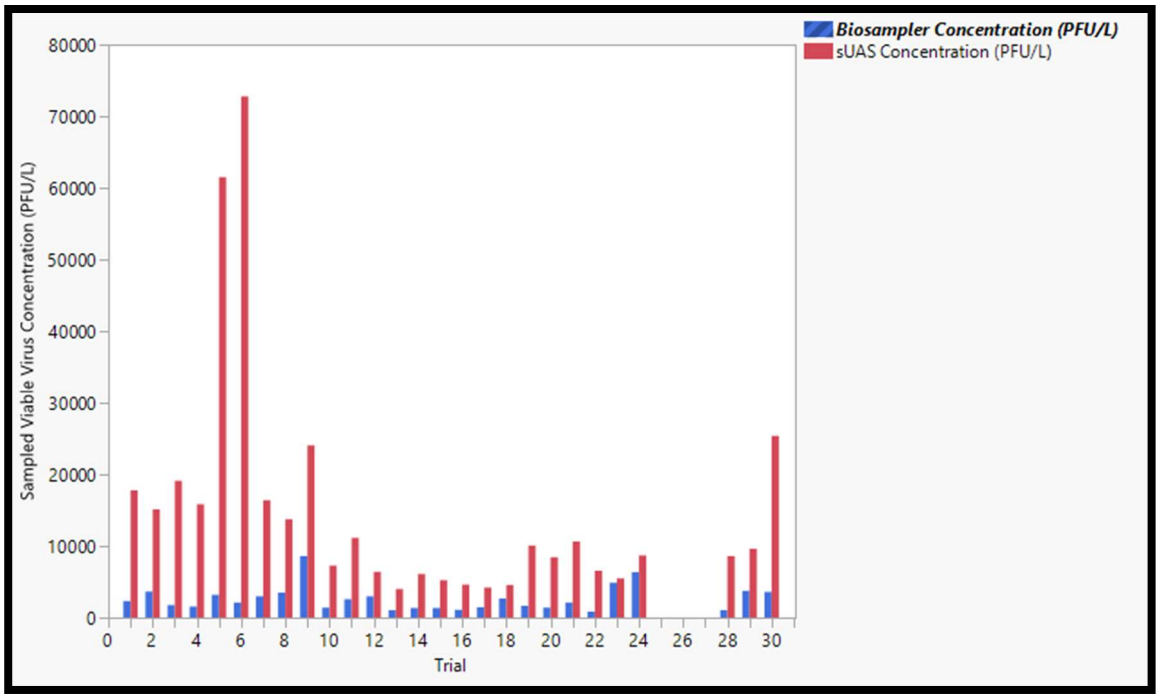

Figure 12. Viable MS2 Air Concentration (PFU/L) by Trial

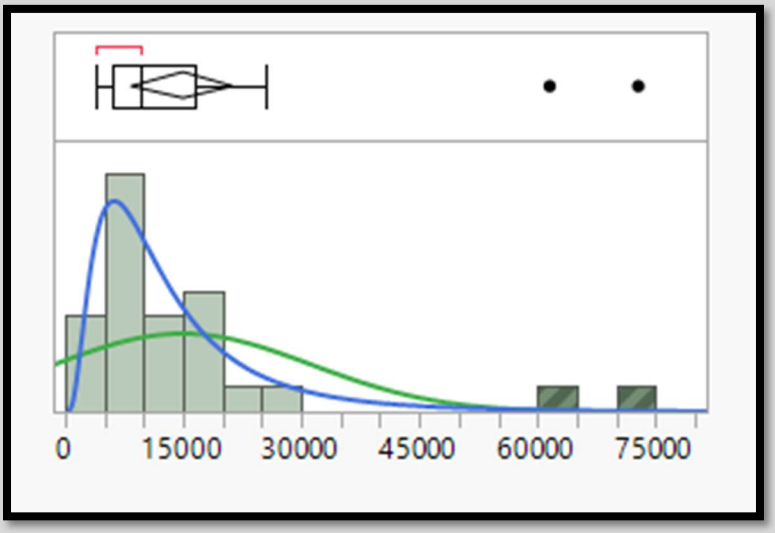

Anderson-Darling Probabilities

Normal Distribution (Green)	<0.0001
Lognormal Distribution (Blue)	0.1610

Figure 13. sUAS Data Goodness-of-Fit Tests

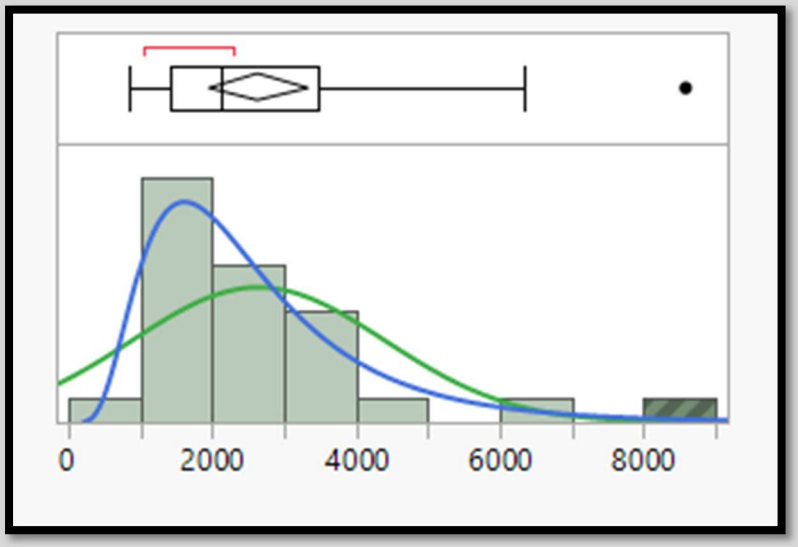

Anderson-Darling Probabilities

Normal Distribution (Green)	<0.001
Lognormal Distribution (Blue)	0.58

Figure 14. Biosampler® Data Goodness-of Fit Tests

Conventional statistical outlier diagnostic tests were not performed due to not satisfying the underlying assumptions of normality. Further, as the sample distributions are acceptably described by a lognormal distribution, several high values comprise the tails of the distribution and may represent valid data points. Therefore, the Interquartile Range (IQR) method was used to identify potential outliers. These points were flagged as outside of the lower and upper fences as shown in Equations 7 and 8 (Ibe, 2014). Potential outliers are represented by dots on the box and whisper plots depicted in Appendix E, Figures E1 and E2. This method identified trials 5, 6, and 9 as containing probable outliers for one of the paired samples (samples 5 and 6 of the sUAS-mounted sampler and sample 9 of the Biosampler®). Conclusive indications for the probable outliers could not be determined. High relative humidity recorded for these trials was

considered as a partial explanation, though logistic regression of this variable on the response failed to produce statistically significant results. As the data points could not definitively be considered valid samples nor outliers, analysis with and without these data points was accomplished.

$$Lower\ Fence = Quartile\ 1 - (1.5 \times IQR) \quad (7)$$

$$Upper\ Fence = Quartile\ 3 + (1.5 \times IQR) \quad (8)$$

Where

Quartile 1 = Median of the Lower Half of Data Set

Quartile 3 = Median of the Upper Half of Data Set

IQR = Difference between Quartile 3 and Quartile 1

Next, air concentrations of viable MS2 could be directly compared between the two samplers. This comparison was achieved through the relative BSE calculation as illustrated in Equation 9. The equation comprises a ratio where the Biosampler® concentration represents the denominator reference point of 100% efficiency. Full results for relative BSE may be found in Appendix D, Table D1.

$$Relative\ BSE = \frac{sUAS\ Concentration}{Biosampler\ Concentration} \quad (9)$$

Where

Relative BSE = Unitless ratio, Relative biological sampling efficiency

sUAS Concentration = PFU/L, corrected for ambient conditions

Biosampler® Concentration = PFU/L, corrected for ambient conditions

Distributions of the relative BSE were evaluated with differing exclusions for outliers. Both sets excluded data points 25-27 as anomalous non-detect data points.

Exclusions and results are displayed in Table 3. Anderson-Darling goodness-of-fit tests were also accomplished on the relative BSE values for both sets of data. These results are displayed in Figures 15 and 16. With the probable outliers and non-detect samples excluded, the relative BSE results are acceptably described by a normal distribution. Thus, a 95% confidence interval could be calculated around the arithmetic mean.

For the second data set that only excluded the non-detect samples, the Anderson-Darling goodness-of-fit test produced a significant p-value of less than 0.05, signaling rejection of the null hypothesis of a normal distribution. The lognormal fit produced a high, non-significant p-value indicating failure to reject the null hypothesis of a lognormal distribution. The BSE results for this data set were then log-transformed. A subsequent Anderson-Darling goodness-of-fit produced a non-significant p-value for a normal fit, prompting failure to reject the null hypothesis of a normal distribution. A 95% confidence interval was calculated around the arithmetic mean of the log-transformed values. These results were then reconverted to the original distribution using the antilog of the log-transformed values. Thus, the 95% confidence interval surrounded the geometric mean (GM) of the second data set.

Results with excluded potential outliers indicate a mean relative BSE of 4.98. Results with no potential outlier exclusions yield a GM relative BSE of 4.82. A 95% confidence interval around the mean and GM relative BSE was also calculated for each of these distributions. Data absent potential outliers yielded an upper bound of approximately 6.1 and a lower bound of 3.9, while data including potential outliers showed an upper bound of 6.5 and lower of 3.6. This can be interpreted that there is 95% confidence the true mean or geometric mean relative BSE will fall within these values.

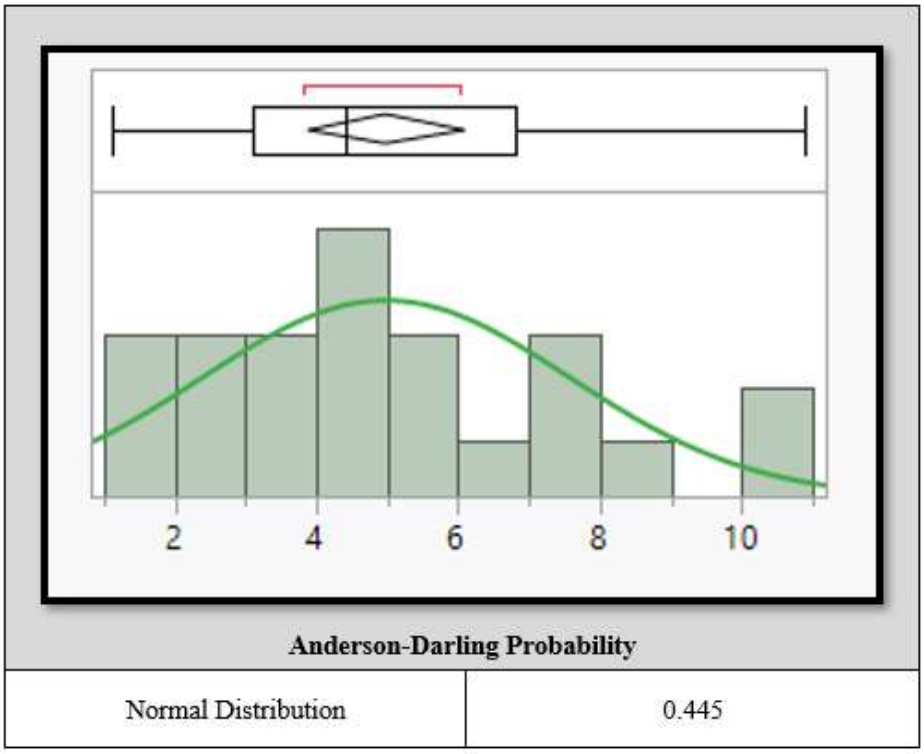

Figure 15. Relative BSE Data Goodness-of-Fit (Excluding Samples 5, 6, 9, 25-27)

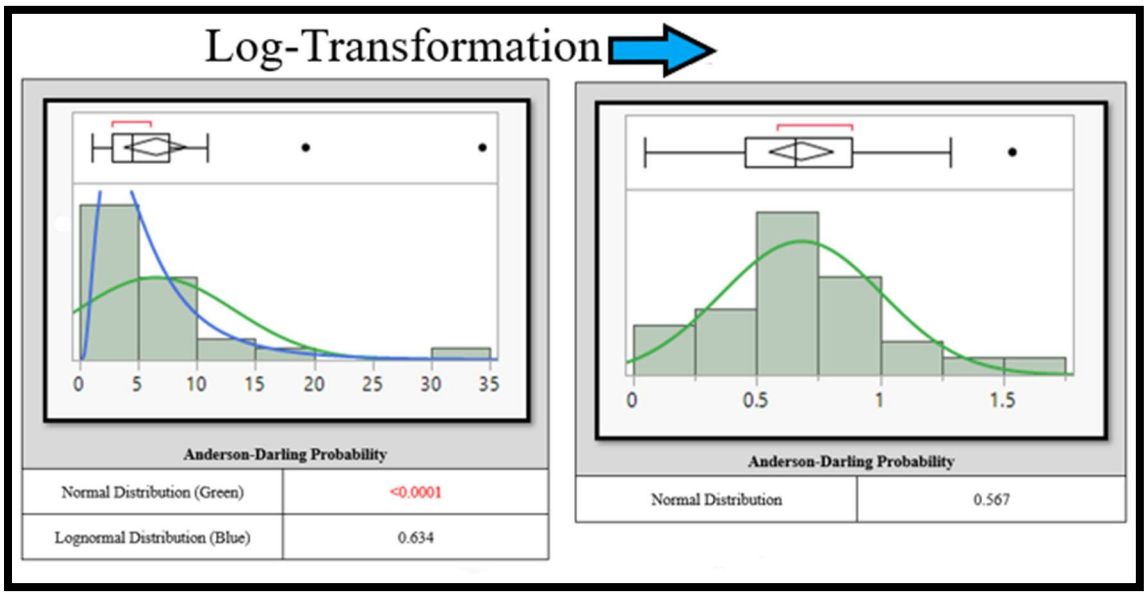

Figure 16. Relative BSE Goodness-of-Fit Before and After Log-Transformation

(Excluding Samples 25-27)

Table 3. Mean Relative BSE Results with 95% Confidence Interval

Excluded Data Points	Mean Relative BSE	Lower Bound 95% Confidence Interval	Upper Bound 95% Confidence Interval
5, 6, 9, 25, 26, 27	**4.98**	3.9	6.1
25, 26, 27	**4.82 (GM)**	3.6	6.5

The difference in means was also tested statistically with a Wilcoxon Signed-Rank test. This test used the mean relative BSE null hypothesis of 1 to indicate no difference in the mean for each sampling device. Results of the two-sided test in Figure 17 yielded a significant p-value of <0.0001, indicating rejection of the null hypothesis that the mean relative BSE is equal to 1.

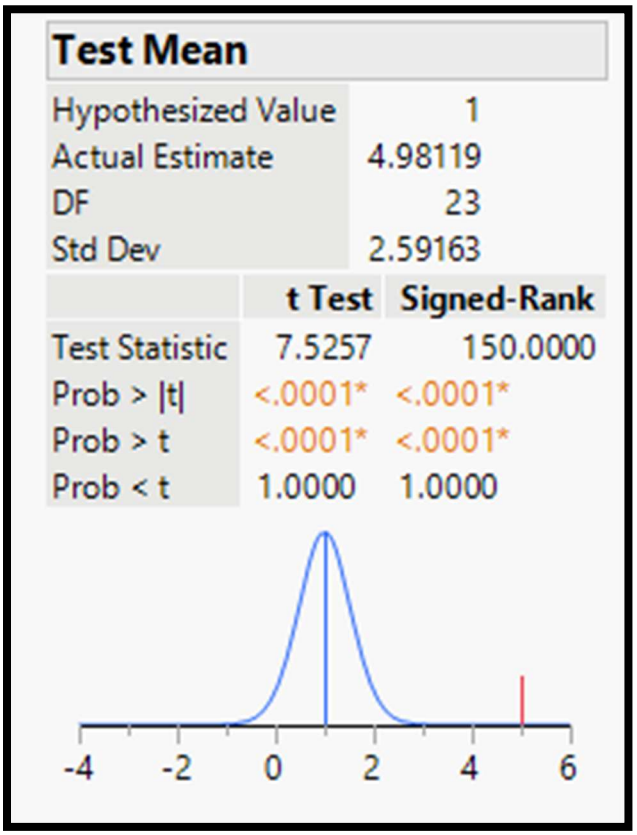

Figure 17. Test Mean Relative BSE

Hence, the null hypothesis of the samplers having an equivalent relative BSE should be rejected. Furthermore, the test shows the mean relative BSE is greater than 1. Therefore, it can be interpreted that the sUAS-mounted sampler with gelatin filters has demonstrably outperformed the Biosampler® in the collection of viable airborne MS2 per liter of air collected, under these experimental conditions. Additional non-parametric statistical tests using intervals of differences in means may be found in Appendix K.

Investigative Questions Answered

The results of this study conclusively answered both investigative questions. First, viable airborne MS2 was reliably collected via gelatin filters affixed to the sUAS in simulated flight as demonstrated by confirmatory plaque assay results. Secondly, the BSE across 24 trials showed consistently superior performance of the sUAS against the Biosampler® for the collection of viable MS2 per liter of air sampled.

Sources of Uncertainty

Uncertainty associated with the experimental setup and analysis should be considered when interpreting BSE results. There were several sources of uncertainty that may have caused positive or negative biases. These are illustrated in Table 4. First, the sUAS-mounted aerosol sampler is open-faced and was positioned face-up during experimentation. This construction may have allowed MS2-containing particles to settle on the filter face during the pre-sampling, 5-minute aerosolization period as well as during sampling. This effect is thought to have a low overestimation of the BSE. The turbulent air from the rotor mixing and non-laminar lateral flow of the chamber should

reduce particle setting rates. Moreover, a large proportion of particles generated by the Collison nebulizer are inert and do not contain any viable virus (Zuo et al, 2014).

Secondly, there may have been residual airborne MS2 particles from previous trials when experiments were run in succession. These residual virions could overestimate concentrations of either device. Purge times of 5-minutes were established based on precedent from Harvey (2022) and Fuller (2022) as adequate times to reduce nebulized bioaerosols to background levels. Quantitative measurements were not taken to confirm this to be true.

Additionally, particles within the chamber that had settled from prior experiments could possibly become re-aerosolized in subsequent trials as chamber decontamination between every trial was not opted for due to time constraints. For very small particles, this is unlikely due to the attractive forces between surfaces and particulates. Larger particles over 20 microns could have become re-aerosolized and contributed to this effect, though the measured particle size distribution shows that larger particles in this size range were seldom present.

These biases from residual MS2 (either still airborne or re-aerosolized) were evaluated statistically using non-parametric one-way analysis of the concentration in PFU/L by run order of either 1, 2, or 3. The Kruskal-Wallis Rank Sums test did not yield a significant outcome ($p =$ for the sUAS-mounted sampler concentrations by run order. This indicates failure to reject the null hypothesis of no difference in responses. ($p = 0.64$). For the Biosampler®, the Kruskal-Wallis test revealed significant results ($p = 0.05$), indicating rejection of the null hypothesis of no difference in responses. Following this, a non-parametric Steel-Dwass All Pairs Comparison was conducted on for the Biosampler®

concentrations by run order. Test outcomes revealed there were statistically significant differences in responses between run order 1 and run order 3. The full results of these tests (with and without probable outliers) may be found in Appendix L. As the sUAS-mounted sampler results were not significantly influenced by these residual MS2 biases from run order, it may be inferred that the actual relative BSE has been underestimated, thus the sUAS-mounted sampler likely outperformed the Biosampler® to a higher degree.

Furthermore, inter-assay variability could have caused an over- or under-estimation of the BSE. The plaque assay process contains many manual steps subject to slight variations each time they are performed. These small variations may lead to significant differences in concentrations obtained through this analysis.

In addition, the MURPHEE chamber dimensions were prohibitive of a parallel sampler setup. Therefore, the samplers were arranged in series with the sUAS-mounted sampler closer to the point of MS2 aerosol generation. This setup could have resulted in either a positive or negative bias of low to medium magnitude for the BSE. While in operation, the sUAS rotors produced well-mixed conditions as characterized by Ohms (2020). Thus, good mixing of aerosolized MS2 likely reduced positional bias effects. Positional effects using an alternate series arrangement were evaluated in a pilot test. The only difference in this alternate arrangement was the transposing of the Biosampler® and sUAS positions. Under these conditions, recovered viable MS2 was non-detect. These results were thought to be at least partially attributed to the position of the devices as the reverse order yielded viable virus results.

Lastly, the notion of inherent underestimation of plaque assay concentration results could have caused either an over- or underestimation of the BSE. This

phenomenon of more than 1 virion within a single plaque noted by Teunis, Lodder, Heisterkamp & de Roda Husman (2005) may be present within MS2 plaques, though this has not been confirmed.

Table 4. Sources of Uncertainty

Assumption/ Source of Uncertainty	Potential Magnitude for OVER-Estimation of BSE	Potential Magnitude for UNDER-Estimation of BSE	Potential Magnitude for "OVER" or "UNDER"	Justification/ Reasoning
Open face & face-up configuration of sUAS Sampler during sampling period & pre-aerosolization	Low	-	-	Turbulent and lateral airflow should slow the settling of small particles substantially resulting in minimal settling on the filter prior to the sampling period.
Residual MS2 concentration from prior trial when run in succession		Low/Medium	-	5-minute purge time was utilized to clear chamber (Harvey, 2022; Fuller, 2022). Return to background concentrations were not verified with direct measurement. Statistical evaluation shows higher concentration for the third sample run in succession only for the Biosampler. Thus, there is an underestimation of the relative BSE.
Inter-assay variability	-	-	Low	Slight variations in the manual process could result in more or less effective assays.
Positional bias of sampling equipment	-	-	Low/Medium	The chamber dimensions precluded parallel set-up. sUAS sampler was closer to the point of generation, though rotors in operation should have maintained well-mixed conditions (Ohms, 2020).
Plaque Assay Underestimation if more than one virus within one plaque	-	-	Low/Medium	Based on findings from Teunis, Lodder, Heisterkamp, de Roda Husman (2005). More than one MS2 virion may have been present within 1 plaque. This has not been confirmed in the literature.

V. Conclusions and Recommendations

Chapter Overview

This chapter summarizes the findings of this study. Additionally, the significance of this research is described in the context of biological defense capabilities. Finally, recommendations for action and future research are established.

Conclusions of Research

The sUAS has proven to be a feasible platform for sampling viral aerosols in a semi-controlled laboratory setting. The selected gelatin filter media successfully captured and preserved viable MS2 virions for analysis by plaque assay. Results of this study determined the mean relative BSE of the sUAS-mounted aerosol sampler to the Biosampler® in the collection of viable MS2 bacteriophage per liter of air sampled to be 4.98 (95% CI 3.9, 6.1), under these experimental conditions and with probable outliers and non-detect samples excluded.

Significance of Research

This research details the novel active aerial sampling of viral aerosols via an unmanned platform. Moreover, the conclusions of this study echo those of Ohms (2020), Fuller (2022), and Harvey (2022). Together, these studies indicate the sUAS is a multi-capable bioaerosol sampling platform within a semi-controlled laboratory setting.

Limitations of Research

There are several important limitations associated with this research. As discussed in Chapter 3, the surrogate bacteriophage used within this study may be more or less

hardy against environmental and sampling-induced stresses than a target pathogenic virus. As such, interpretations of this study's findings should be limited to the relative BSE of MS2 bacteriophage.

Secondly, as pointed out by Fuller (2022), the sUAS rotor wash and turbulent airflows were amplified by the MURPHEE chamber surfaces. These conditions will greatly differ from an outdoor sampling environment and will almost certainly have an effect on sampling efficiencies.

Recommendations for Action

The sUAS should be further engineered to have an onboard battery system minimally capable of powering flight and sampling systems for 15 minutes. Small camera systems for concurrent reconnaissance activities should also be considered, noting added weight and power requirements and the related effects on flight times.

Recommendations for Future Research

Future research should continue inquiry into viral sampling capabilities. Several factors could be explored in more depth including viability losses associated with sampling, the performance of other media types in the collection of viral aerosols, and flow rate effects on BSE.

Complementing analytical techniques such as qPCR and plaque assay could be used to evaluate total virions against viable virions sampled. These parallel techniques could reveal viability losses associated with aerosolization and collection on filter media.

Other media types should also be evaluated for the collection of MS2 bacteriophage against gelatin filters to isolate the effects of desiccation associated with

the selected sampling media. Polytetrafluoroethylene (PTFE) filters, in particular, showed very high PSE of MS2 bacteriophage (Burton et al., 2007). PSE as well as BSE should be evaluated using the sUAS-mounted sampler.

As stated by Fuller (2022) and Harvey (2022), a redesign of the sUAS-mounted sampler should be considered for future research including a closed filter face configuration and an increase in flow rate potential. This author supports those assertions. Specifically, an evaluation of flow rate effects on BSE may be warranted. The caveat for such an evaluation of higher flow rates (hence total air volumes) for the sUAS is the filter media must not be as predisposed to desiccation effects as was seen in gelatin materials.

Finally, passive sampling of both bacteria and viruses should be explored. These methods proved successful for other sUAS bioaerosol applications and may provide a time and resource-efficient biological agent detection sampling capability. Active and passive methods could be paired on the same platform to assess the ability of both techniques for presumptive identification via field analytical equipment, such as PCR and lateral flow antibody-antigen tests.

Numerous characterizations would allow a better understanding of the strengths and weaknesses of the many available sampling configurations to support both targeted and unknown bioaerosol sampling. To quote Dybwad, Skogan, and Blatny (2014),"…no single air sampler will be universally optimal, or even suitable, for all bioaerosols and bioaerosol sampling purposes."

Summary

Innovations in biological sampling equipment and techniques are essential to meeting the goals and objectives of the NBSIP. The DoD's investment in this research space will propel its unmanned bioaerosol sampling capabilities, ultimately supporting timely data acquisition and risk reduction.

Appendix A. Raw Results

Table A1. Plaque Assay Results, Trials 1-15

Trial	Device	Total PFU	Liquid Matrix Volume (mL)	Assay Result (PFU/mL)
1	Biosampler	399840	17.5	22848
	sUAS	161220	20	8061
2	Biosampler	635994	18	35333
	sUAS	136960	20	6848
3	Biosampler	305442	18	16969
	sUAS	173340	20	8667
4	Biosampler	271757	19	14303
	sUAS	138340	20	6917
5	Biosampler	551570	19	29030
	sUAS	535760	20	26788
6	Biosampler	365028	19	19212
	sUAS	631520	20	31576
7	Biosampler	517050	18.75	27576
	sUAS	145460	20	7273
8	Biosampler	596486	19	31394
	sUAS	121220	20	6061
9	Biosampler	1469327	19	77333
	sUAS	212120	20	10606
10	Biosampler	241813	19	12727
	sUAS	64960	20	3248
11	Biosampler	441761.5	18.5	23879
	sUAS	99400	20	4970
12	Biosampler	511271	19	26909
	sUAS	57060	20	2853
13	Biosampler	182962.5	18.75	9758
	sUAS	36500	20	1825
14	Biosampler	233757	19	12303
	sUAS	55020	20	2751
15	Biosampler	234916	19	12364
	sUAS	47340	20	2367

Table A2. Plaque Assay Results, Trials 16-30

Trial	Device	Total PFU	Liquid Matrix Volume (mL)	Assay Result (PFU/mL)
16	Biosampler	188730	18	10485
	sUAS	40480	20	2024
17	Biosampler	253406.3	18.75	13515
	sUAS	36620	20	1831
18	Biosampler	461757	19	24303
	sUAS	39760	20	1988
19	Biosampler	290178	18	16121
	sUAS	88480	20	4424
20	Biosampler	242190	18	13455
	sUAS	73980	20	3699
21	Biosampler	368730	18	20485
	sUAS	93340	20	4667
22	Biosampler	149454	18	8303
	sUAS	59060	20	2953
23	Biosampler	849993.8	18.75	45333
	sUAS	49480	20	2474
24	Biosampler	1103994	18	61333
	sUAS	78280	20	3914
25	Biosampler	Non-Detect	19	Non-Detect
	sUAS	Non-Detect	20	Non-Detect
26	Biosampler	Non-Detect	19	Non-Detect
	sUAS	Non-Detect	20	Non-Detect
27	Biosampler	Non-Detect	18.5	Non-Detect
	sUAS	Non-Detect	20	Non-Detect
28	Biosampler	191159	19	10061
	sUAS	91720	20	4586
29	Biosampler	667339.8	19.25	34667
	sUAS	102560	20	5128
30	Biosampler	640243	19	33697
	sUAS	270300	20	13515

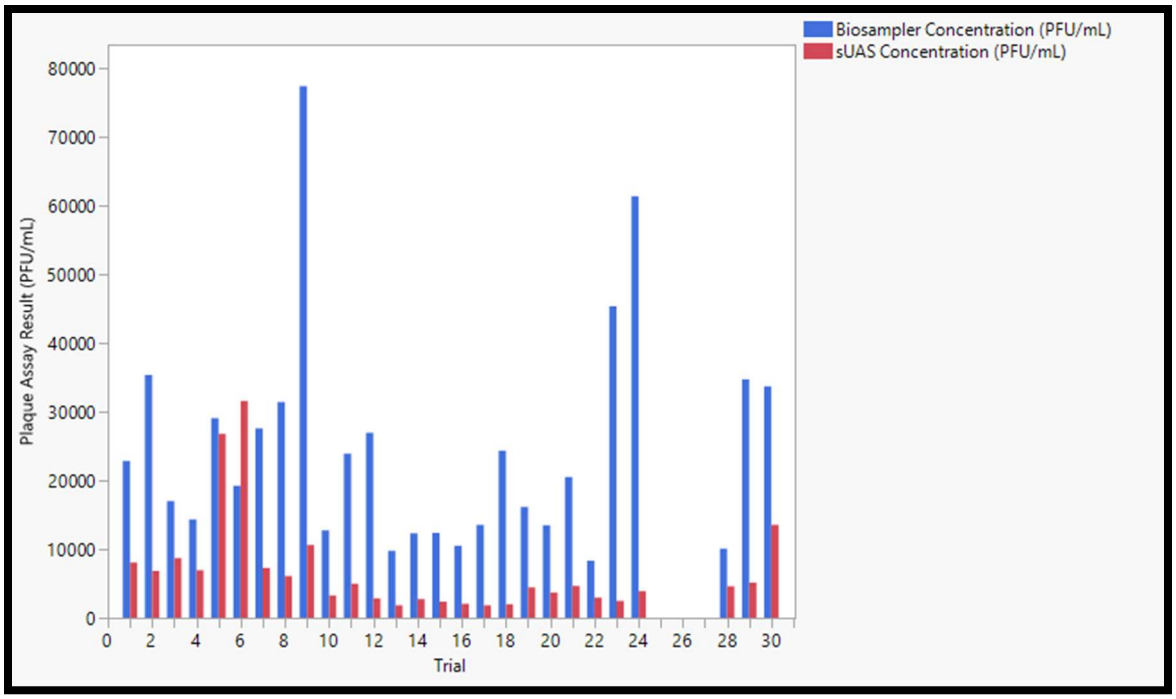

Figure A1. Plaque Assay Results (PFU/mL) by Sampling Device

Appendix B. Calibration Data

Table B1. Calibration Data

Trial	Device	Pre-Calibration Flow Rate (lpm)	Post-Calibration Flow Rate (lpm)	Flow Rate Difference (%)	Average Flow Rate (lpm)
1-3	Biosampler	12.003	12.005	0.02	12.004
	sUAS	0.631	0.622	-1.43	0.6265
4-6	Biosampler	12.031	12.011	-0.08	12.021
	sUAS	0.604	0.606	0.33	0.605
7-9	Biosampler	12.01	11.972	-0.32	11.991
	sUAS	0.614	0.62	0.98	0.617
10-12	Biosampler	12.016	12.002	-0.12	12.009
	sUAS	0.628	0.626	-0.32	0.627
13-15	Biosampler	12.019	12.007	-0.1	12.013
	sUAS	0.64	0.612	-4.38	0.626
16-18	Biosampler	12.003	12.002	-0.01	12.0025
	sUAS	0.616	0.608	-1.3	0.612
19-21	Biosampler	12.01	12.004	-0.05	12.007
	sUAS	0.615	0.606	-1.46	0.6105
22-24	Biosampler	12.039	12.027	-0.1	12.033
	sUAS	0.622	0.627	0.8	0.6245
25-27	Biosampler	12.023	12.017	-0.05	12.02
	sUAS	0.608	0.602	-0.99	0.605
28-30	Biosampler	12.043	12.029	-0.12	12.036
	sUAS	0.721	0.717	-0.55	0.719

Appendix C. Sample Volume Corrections

Table C1. Sample Volumes Corrected with Temperature and Pressure

Trial	Device	Uncorrected Sample Volume (L)	Measured Temperature (K)	Ambient Pressure (atm)	Corrected Sample Volume (L)
1	Biosampler	180.06	298	0.97	173.76
	sUAS	9.40			9.07
2	Biosampler	180.06	298	0.97	173.76
	sUAS	9.40			9.07
3	Biosampler	180.06	298	0.97	173.76
	sUAS	9.40			9.07
4	Biosampler	180.32	299	0.97	173.60
	sUAS	9.08			8.74
5	Biosampler	180.32	300	0.97	173.02
	sUAS	9.08			8.71
6	Biosampler	180.32	301	0.97	172.45
	sUAS	9.08			8.68
7	Biosampler	179.87	301	0.97	172.37
	sUAS	9.26			8.87
8	Biosampler	179.87	303	0.97	171.24
	sUAS	9.26			8.81
9	Biosampler	179.87	303	0.97	171.24
	sUAS	9.26			8.81
10	Biosampler	180.14	303	0.97	171.14
	sUAS	9.41			8.94
11	Biosampler	180.14	303	0.97	171.14
	sUAS	9.41			8.945
12	Biosampler	180.14	303	0.97	171.14
	sUAS	9.41			8.94
13	Biosampler	180.20	300	0.97	174.16
	sUAS	9.39			9.08
14	Biosampler	180.20	301	0.97	173.58
	sUAS	9.39			9.05
15	Biosampler	180.20	301	0.97	173.58
	sUAS	9.39			9.05
16	Biosampler	180.04	303	0.97	171.40
	sUAS	9.18			8.74
17	Biosampler	180.04	303	0.97	171.40
	sUAS	9.18			8.74
18	Biosampler	180.04	304	0.97	170.84
	sUAS	9.18			8.71
19	Biosampler	180.11	301	0.97	172.78
	sUAS	9.16			8.79
20	Biosampler	180.11	302	0.97	172.21
	sUAS	9.16			8.76
21	Biosampler	180.11	301	0.97	172.78
	sUAS	9.16			8.79
22	Biosampler	180.50	301	0.97	173.87
	sUAS	9.37			9.02
23	Biosampler	180.50	301	0.97	173.87
	sUAS	9.37			9.02
24	Biosampler	180.50	301	0.97	173.87
	sUAS	9.37			9.02
25	Biosampler	180.3	297	0.98	176.38
	sUAS	9.08			8.88
26	Biosampler	180.3	298	0.98	175.79
	sUAS	9.08			8.85
27	Biosampler	180.3	299	0.98	175.21
	sUAS	9.08			8.82
28	Biosampler	180.54	302	1.00	178.68
	sUAS	10.79			10.67
29	Biosampler	180.54	302	1.00	178.68
	sUAS	10.79			10.67
30	Biosampler	180.54	303	1.00	178.09
	sUAS	10.79			10.64

Appendix D. Relative BSE

Table D1. Relative BSE Results

Trial	Biosampler® Concentration (PFU/L)	sUAS Concentration (PFU/L)	Rel. BSE
1	2301.13	17777.85	7.73
2	3660.23	15102.68	4.13
3	1757.86	19114.33	10.87
4	1565.40	15833.57	10.11
5**	3187.84	61524.98	19.30*
6**	2116.74	72763.50	34.38*
7	2999.58	16399.93	5.47
8	3483.41	13757.80	3.95
9**	8580.70*	24074.44	2.81*
10	1412.96	7270.03	5.15
11	2581.30	11124.41	4.31
12	2987.46	6385.90	2.14
13	1050.54	4021.79	3.83
14	1346.66	6082.64	4.52
15	1353.34	5233.59	3.87
16	1101.11	4631.79	4.21
17	1478.45	4190.12	2.83
18	2702.92	4564.42	1.69
19	1679.44	10071.51	6.00
20	1406.36	8448.98	6.01
21	2134.07	10624.72	4.98
22	859.57	6544.96	7.61
23	4888.64	5483.32	1.12
24	6349.49	8674.90	1.37
25*	Non-Detect	Non-Detect	-
26*	Non-Detect	Non-Detect	-
27*	Non-Detect	Non-Detect	-
28	1069.82	8592.78	8.03
29	3734.77	9608.32	2.57
30	3594.98	25406.88	7.07
Mean (potential outliers excluded)			**4.98**
Geometric Mean (with potential outliers)			**4.82**

*Indicates excluded non-detect data points

** Indicates potential outliers

Appendix E. Goodness of Fit and Outlier Assessment

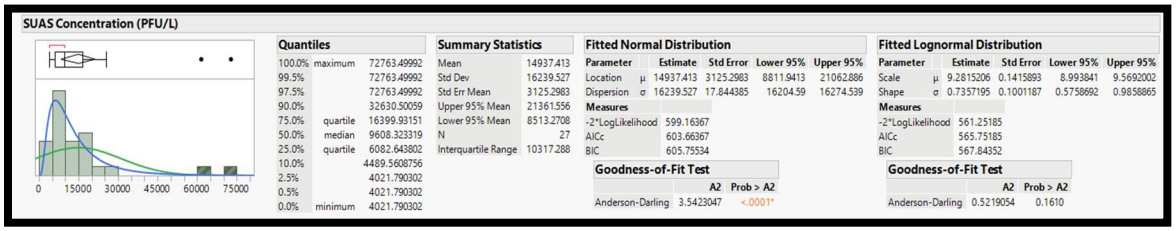

Figure E1. sUAS Concentration (PFU/L) Assessment

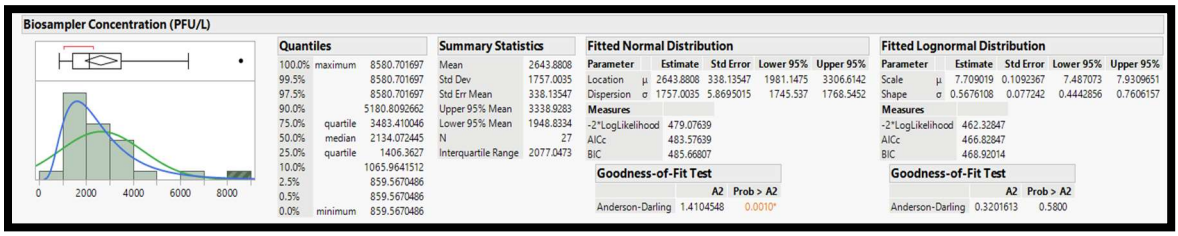

Figure E2. Biosampler® Concentration (PFU/L) Assessment

Appendix F. Recorded Relative Humidity by Trial

Table F1. Relative Humidity by Trial

Trial	Relative Humidity (%)
1	59
2	59
3	59
4	68
5	68
6	69
7	63
8	65
9	64
10	60
11	56
12	53
13	47
14	47
15	47
16	50
17	48
18	49
19	47
20	48
21	48
22	49
23	49
24	48
25	51
26	50
27	48
28	63
29	63
30	63

Appendix G. Phage Stock Titer Results and Aerosolization Concentration

Table G1. Phage Stock and Aerosolization Concentrations

Titer Identifier	Phage Stock Concentration (PFU/mL)	Aerosolization Solution Concentration (PFU/mL)
Pre-Experimentation	2.799E11	2.799E10
Mid-Point	7.82E10	7.82E09
Post-Experimentation	2.01E11	2.01E10

Appendix H. Step-by-Step Aerosolization and Sampling Protocol

MS2 Aerosolization and Sampling Procedures

Materials Needed:

- Filtered MS2 Stock
- Sterile Deionized Water
- Sterile 50 mL Conical Tubes
- Parafilm®
- Aluminum Foil
- Cooler
- Ice Packs
- Biological Material Bags
- Autoclave Bags
- Autoclave Tape
- Disposable Nitrile Gloves
- Sterile Pipettes
- Collison nebulizer
- Eye Protection
- Lab Coat
- HEPA Filter
- PFTE Tubing
- Sterile Forceps
- SKC Gelatin Filters
- 1X PBS (20 mL per sample)
- Lint Free Paper Towels
- Clorox Fuzion®

General Notes Before Beginning:

The Biosampler® and Collison nebulizer should be sterilized and cooled prior to aerosolization. Per the manufacturer, the Collison nebulizer is autoclave safe. This is the preferred method to avoid potential bleach residue. Alternatively, the Collison nebulizer may be submerged in 10% bleach solution for 15 minutes then submerged and thoroughly rinsed in sterile deionized water.
The tubing ends become stretched after repeated use. Small segments should be cut from the end of the tubing to prevent disconnection during aerosolization.
Transport of MS2 in a cooler should be restricted to transit only to ensure storage temperatures do not exceed 4 degrees Celsius, which increases the risk of loss of the

phage's viability. Once at the research facility, the phage should be placed in the designated BSL-1 refrigerator until use.

Aerosolization Solution Preparation Procedures:

1. Don gloves, eye protection, and lab coat prior to handling phage.
2. Prepare 10 percent phage solution using 36 mL of sterile deionized water and 4 mL filtered phage stock. Store in 50 mL sterile conical tube.
3. Apply a thin strip of Parafilm® in a clockwise motion to ensure lid is not inadvertently loosened.
4. Wrap tube(s) in aluminum foil.
5. Place wrapped tube(s) in Biohazard bag.
6. Place bag(s) in cooler with several ice packs.
7. Transport to phage stock from laboratory to research facility

MURPHEE Preparation Procedures:

1. Turn on power to MURPHEE fan.
2. Set MURPHEE chamber airflow fan setting to 16.0 Hz (0.2 m/s)
3. Open access door and secure in open position using metal clasp.
4. Spray all inside surfaces of chamber with Clorox Fuzion® disinfectant.
5. Allow disinfectant to contact for at least 15 minutes.
6. Wipe off residue using lint-free paper towel and deionized water.
7. Close MURPHEE access door until experimentation to prevent contamination from entering.

Pre-Calibration Procedures:

1. Record time, date, temperature, and pressure.
2. Fill calibration Biosampler® with 20 mL deionized water.
3. Connect Biosampler® to Mesa Labs Dry Cal Calibrator inlet port via PFTE tubing.
4. Connect calibrator outlet port to Biolite high-volume pump.
5. Turn on Biolite high-volume pump.
6. Set Mesa Labs calibrator to continuous setting. Adjust Biolite pump with knob to 12 lpm.
7. Change calibrator setting to burst.
8. Initiate burst sequence. Record the average of 10 measurements.
9. Connect sUAS pump to calibration chain with representative filter media to replicate pressure drop.
10. Secure calibration cap with zip ties on opposite sides of the cap.

11. Ensure orientation of airflow from sampling pump through TSI 4100 series flow-through meter is in correct direction. Reference the arrow on the TSI 4100 series flow-through meter
12. Turn on in-line flow meter.
13. Connect sUAS fan to power source. Fan should automatically start,
14. Allow several seconds for flow to equilibrate.
15. Take 3 measurements by looking away for several seconds then observing flow reading on TSI flow through meter. Repeat 2 more times.
16. Record the average of the flow rate.

Experimental Setup and sUAS Test Procedures:

1. Open access door to MURPHEE chamber and secure open via the metal clasp.
2. Measure the clamp stand heights and distances in accordance with Figure 6.
3. Thread PFTE tubing through access ports in the side of the MURPHEE chamber for Collison nebulizer in-flow and Biosampler® outflow.
4. Attach air pressure line (with HEPA filter) to ALICAT Mass Flow meter.
5. Turn on air flow and record measurements in liters per minute and psi.
6. Connect HEPA filter to tubing after Biosampler® outlet.
7. Connect outgoing HEPA filter tubing to precision rotameter inlet.
8. Connect tubing to precision rotameter outlet, then to Biolite pump.
9. Seal MURPHEE access ports around tubing with duct tape to prevent air leaks in chamber.
10. Place sUAS within MURPHEE chamber directly in front of access door.
11. Secure sUAS mount with lead brick.
12. Connect sUAS servo driver cable to servo driver outside of the MURPHEE chamber via access ports.
13. Thread external power cord through access port. Do not connect sUAS at this point to power source.
14. Duct tape gaps around the cables at access ports to prevent air leaks.
15. Plug in servo driver via 110V connection.
16. Connect external power cables to voltage converter.
17. Adjust course voltage to 16V via the course dial.
18. Depress the green button to turn on power.
19. Ensure clearance of sUAS rotors. Plug in to sUAS power source
20. Adjust servo driver to 1400 µs rotor speed in manual mode via dial.
21. Ensure all rotors are active. If one or more do not initiate, turn rotor setting to 0 and disconnect sUAS from external power. In this event, take sUAS to ANT center for servicing.
22. If all rotors initiate as expected, reduce rotor speed to 0 and disconnect from external power source.

Aerosolization Solution Setup Procedures:

1. Don appropriate personal protective equipment.
2. Vortex 50 mL conical tube containing phage solution for 5 seconds to thoroughly homogenize.
3. Pour tube into Collison nebulizer reservoir.
4. Place contaminated tube in autoclave bag.
5. Secure top section of nebulizer by screwing clockwise.
6. Secure Collison nebulizer to in MURPHEE chamber at designated height.
7. Secure tubing to Collison nebulizer using electrical tape to prevent disconnection.
8. Adjust depth of metal inlet approximately 1 cm below the level of solution. Higher depths may result in inconsistent aerosol stream due to decreasing solution levels throughout the trial.

Sampler Setup:

1. Don new gloves
2. Add 20 mL 1x PBS to sterile Biosampler® Reservoir.
3. Attach top half of Biosampler® along with inlet component.
4. Secure Biosampler to clamp stand in MURPHEE chamber.
5. Ensure orientation of Biosampler® inlet faces towards Collison outflow near midline of the chamber.
6. Don new gloves
7. Remove gelatin filters from cold storage.
8. Stage sterile 3-component filter holder.
9. Using sterile forceps, remove gelatin filter from packaging and place fibrous side up onto filter holder base.
10. Secure filter with cap taking care not to crack filter media. If cracking is observed repeat from step 6.
11. Place inlet cap over filter holder and secure to sUAS sample pump with two bolts and wingnuts. Hand-tighten, taking care not to over tighten.
12. Attach sUAS sampler to top of sUAS body via hook and loop connectors. Ensure sampler outlet facing downstream towards the fan.
13. Close MURPHEE chamber door. Secure seams with duct tape. Ensure all ports are covered using duct tape, to include gaps around in-going tubes.

Experimental Procedures:

1. Connect sUAS to external power.
2. Adjust servo driver to 1400 µs.
3. Turn pressurized airline supply valve to the on position.
4. Set timer for 5 minutes.
5. Monitor for excess foaming, tubing disconnection, and steady aerosol stream.

6. Record temperature, pressure, and relative humidity.
7. After 5 minutes of aerosolization, turn on both the Biosampler® and sUAS.
8. Set sampling timer for 15 minutes.
9. After 15 minutes elapse, turn off Collison nebulizer pressure inflow, sUAS rotors, sUAS sampling pump, and Biosampler® as concurrently as feasible.
10. Allow 5 minutes for chamber to purge airborne virions.

Sample Retrieval Procedures:

1. Don gloves
2. Remove duct tape strips from access door.
3. Open access door and secure via metal clasp.
4. Remove sUAS sampler from the sUAS body.
5. Unscrew wingnuts from bolts.
6. Remove filter holder.
7. Remove filter with sterile forceps.
8. Insert filter into pre-labeled sterile 50 mL conical tube with 20 mL of 1x PBS.
9. Close cap of conical tube.
10. Hand swirl for approximately 30 seconds until filter media is thoroughly dissolved.
11. Record volume of contents.
12. Seal tube with Parafilm®. Place in Biological sample bag and store at 4°C.
13. Don new gloves.
14. Retrieve Biosampler® after disconnecting PFTE tubing from inlet.
15. Hand swirl liquid in reservoir for several seconds.
16. Remove top parts of Biosampler®.
17. Pour contents of reservoir into pre-labeled sterile 50 mL conical tube.
18. Close cap of conical tube.
19. Record volume of contents.
20. Seal tube with Parafilm®. Place in Biological sample bag and store at 4°C.
21. Don new gloves.
22. Retrieve Collison nebulizer after disconnecting inlet tubing.
23. Hand swirl contents briefly.
24. Pour aerosolization solution into pre-labeled sterile 50 mL conical tube.
25. Close cap of conical tube.
26. Record volume of contents.

Post-Calibration Procedures:

1. Record time, date, temperature, and pressure.
2. Repeat steps 2-16 as outlined in *Pre-Calibration Procedures* section.

Clean-Up Procedures:

1. Thoroughly decontaminate MURPHEE chamber using same practice as MURPHEE preparation procedures, reseal chamber and secure all seams and ports with duct tape.
2. Hand wipe sUAS body and mount with Clorox Fuzion® and lint free paper towels. Allow contact of 15 minutes then re-wipe with deionized water.
3. Wrap 2 Collison nebulizer parts separately in aluminum foil and secure with autoclave tape.
4. Wrap Biosampler® components separately in aluminum foil and secure with autoclave tape.
5. Disinfect sUAS filter components by submerging in 10% bleach solution for at least 15 minutes.
6. Submerge sUAS parts in sterile deionized water.
7. Dry parts under UV setting of BSC. Store in sterile bag until use.
8. Place all contaminated disposable items in autoclave biowaste bag and secure with autoclave tape.
9. Autoclave Biosampler® and nebulizer parts and waste separately. Use autoclave setting of 121 degrees Celsius, 15 psi for 30 minutes.

Appendix I. Step-by-Step Aerosolization MS2 Enumeration Procedures

Adapted from Adams (1959) and EPA (2018)

Materials Needed:

- 100 mm disposable Petri dishes
- 1000 uL pipette tips
- 200 uL pipette tips
- Adjustable micro-pipetter
- 60 ml syringe
- 15 ml conical tubes
- 50 ml conical tubes
- 1.5 mL microcentrifuge vials
- 15 mL glass test tubes and metal cap
- 25 mL Autopipette tips
- 5 mL disposable pipette
- 0.22 um MCE filters
- Glass beakers
- Shaker flasks
- Glass jars with screw cap
- Glycerol Stocks of E.coli
- Propagated MS2
- Antibiotic stocks (ampicillin and streptomycin)
- Autoclave Tape
- Aluminum Foil
- Parafilm®
- Disposable Nitrile Gloves
- Disposable Cloth Lab Coats
- Eye Protection with Side Shields
- 70% Ethanol
- Sterile Deionized Water
- Bleach
- Markers
- TSB
- Agar
- Weighing Boats
- 15 mL test tube tack
- Autopipetter

General Notes Before Beginning:
Log Phase Host Culture, MS2 stock, antibiotic stock, and 1.5% TSA bottom layer plates, and serially diluted samples should be prepared in accordance with EPA Method 1643. Stored 1.5% TSA bottom layer plates should be brought to room temperature under the BSC.

BSC Preparation Procedures:

1. Turn on BSC.
2. Open sash to pre-measured operational height.
3. Don gloves, lab coat, and eye protection.
4. Apply 10% bleach solution to work surfaces. Allow 15 minutes of contact time.
5. Wipe clean with sterile deionized water. Allow water to evaporate.
6. Spray 70% ethanol solution onto work surfaces. Spread solution with sterile paper towel and allow to evaporate.
7. Any equipment or supplies entering the BSC should be wiped with ethanol.

0.7% TSA Overlay Procedure:

1. Don appropriate PPE.
2. Using a microbalance, weigh out 7 g Agar and 30 g TSB per 1000 mL deionized water on disposable weighing boats.
3. Add desired amount of deionized water to glass screw-top jar.
4. Slowly add weighed ingredients to the solution while hand swirling.
5. Loosely cap the jar and apply autoclave tape.
6. Autoclave for 30 minutes at 121°C and 15 psi.
7. Cool to approximately 50°C within BSC. Verify temperature with infrared thermometer.
8. Aseptically add antibiotic stock at volume to volume ratio of 10 mL antibiotic stock per 1000 mL TSA.
9. Hand swirl solution.
10. Measure temperature again to ensure molten agar is 48°C +/- 1°C to be below *E. coli* critical temperature.
11. Complete plating in triplicate for each desired serial dilution.
12. Vortex 1.5 mL microcentrifuge tubes containing serial dilution of samples for 5 seconds.
13. Aseptically add 5 mL 0.7% TSA into glass 15 mL test tube using autopipetter with 25 mL tip attached.
14. Inoculate 500 µL serial diluted sample into tube with TSA.
15. Inoculate 100 µL log phase *E. coli* culture into tube with TSA.
16. Angle tube approximately 45 degrees between gloved hands and roll tube to homogenize liquid.

17. Pour tube contents onto prepared bottom layer plate and gently tilt plate in a figure-8 shape to evenly distribute top agar layer.
18. Allow agar plates to cool for approximately 10 minutes within BSC.
19. Cap plates, invert them, and incubate for 16-24 hours at approximately 36°C.
20. Count any formed plaques and annotate with a marker dot to avoid overcounting.
21. Calculate concentration for plates containing 1-200 plaques in accordance with EPA method 1643.

Appendix J. Measured Particle Size Distribution

Table J1. Particle Counts by Bin

Bin	Mean Bin Size -Dopt (µm)	Delta log Dopt	Delta Count	Count/Dopt
C0.3-0.5µm	0.4	0.146128	199926	499815
C0.5-1.0µm	0.75	0.154902	472523	630030.7
C1.0-2.5µm	1.75	0.30103	568419	324810.9
C2.5-5.0µm	3.75	0.39794	97857	26095.2
C5.0-10.0µm	7.5	0.30103	790	105.3333
C>10.0µm	15	0.30103	18	1.2

Appendix K. Matched Pairs Statistical Tests

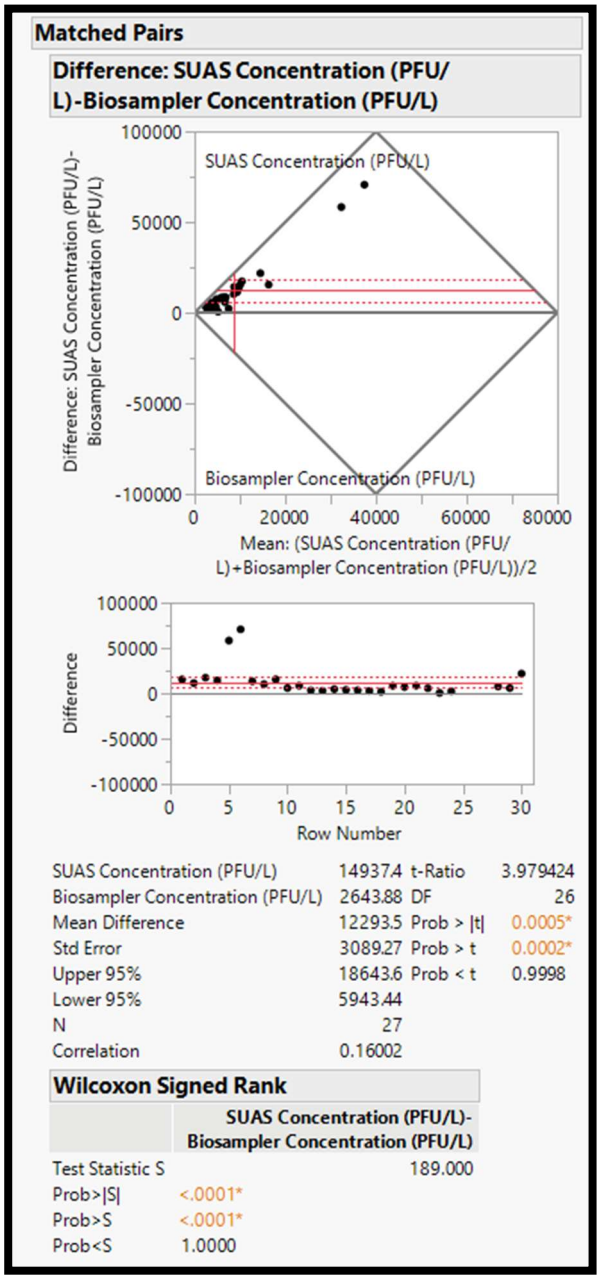

Figure K1. Matched Pairs Assessment (Excluding Trials 25-27)

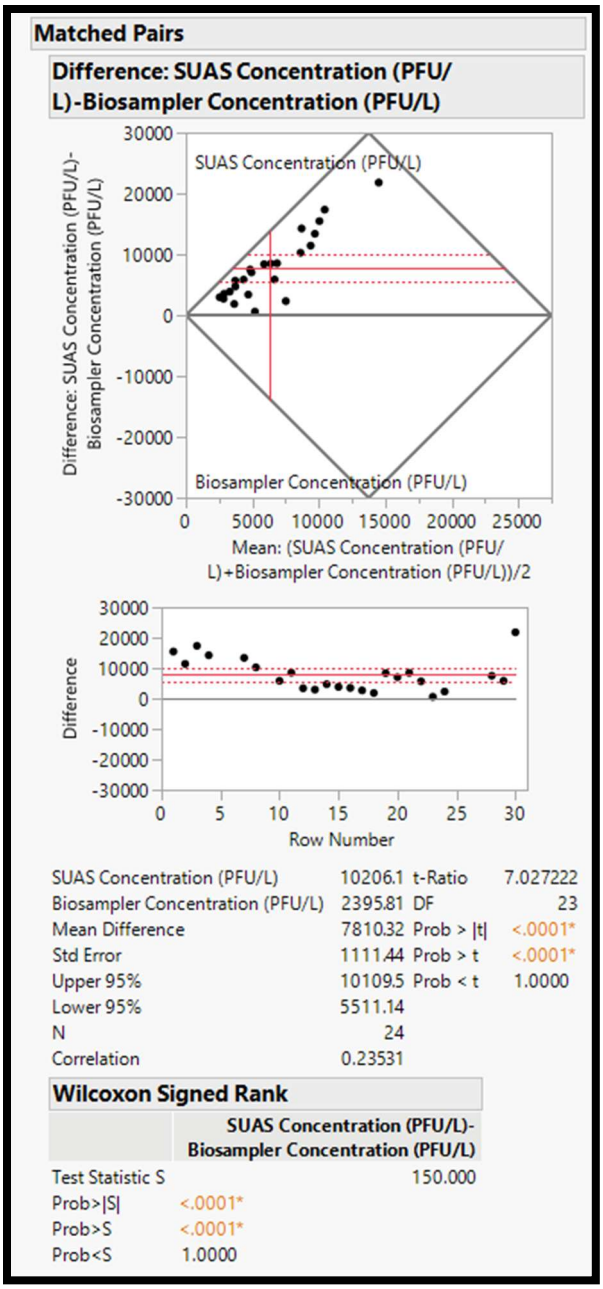

Figure K2. Matched Pairs Assessment (Excluding Trials 5, 6, 9, 25-27)

Appendix L. Residual MS2 Bias by Run Order Assessment

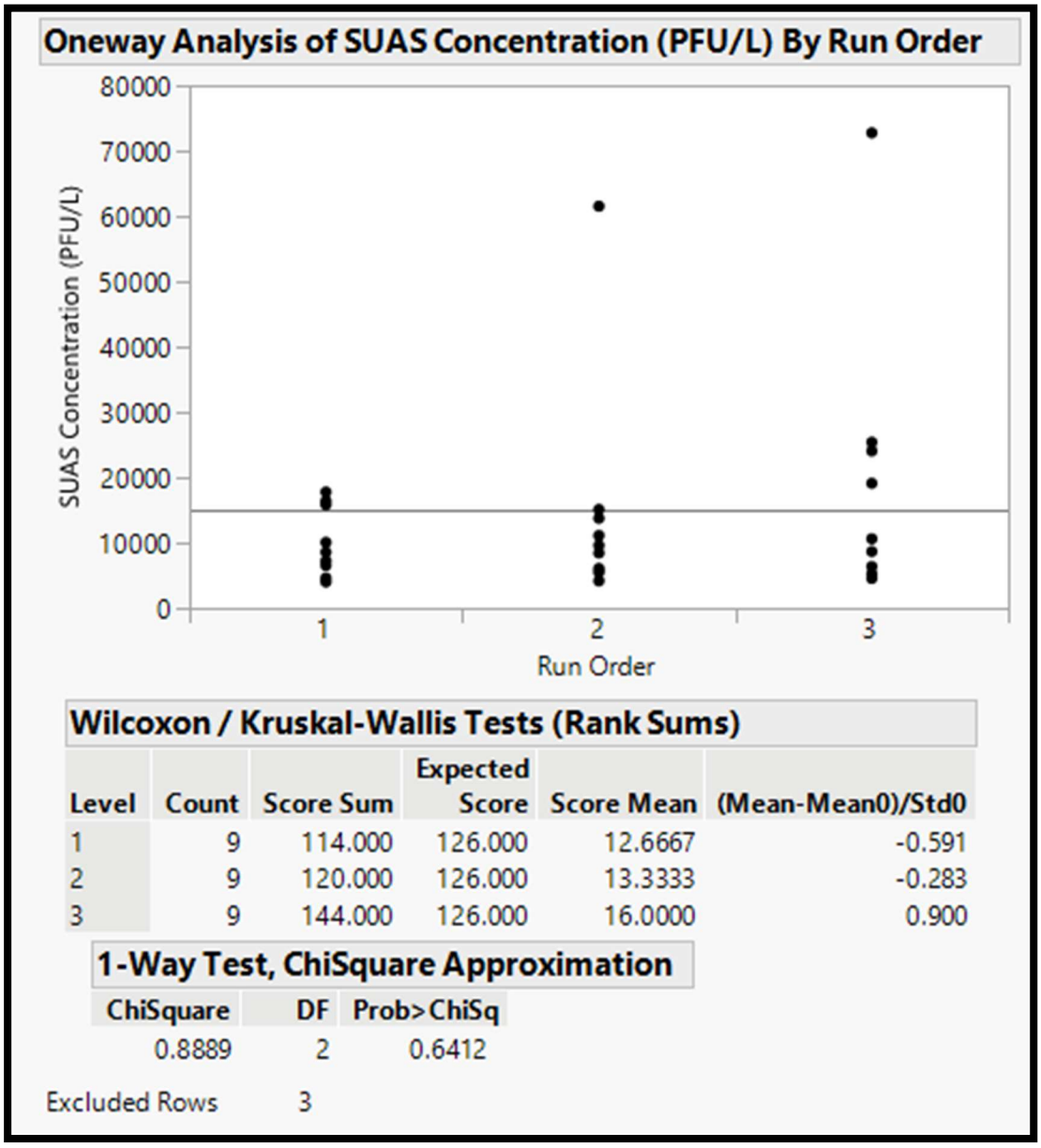

Wilcoxon / Kruskal-Wallis Tests (Rank Sums)

Level	Count	Score Sum	Expected Score	Score Mean	(Mean-Mean0)/Std0
1	9	114.000	126.000	12.6667	-0.591
2	9	120.000	126.000	13.3333	-0.283
3	9	144.000	126.000	16.0000	0.900

1-Way Test, ChiSquare Approximation

ChiSquare	DF	Prob>ChiSq
0.8889	2	0.6412

Excluded Rows 3

Figure L1. One-Way Analysis sUAS-Mounted Sampler Concentration by Run Order

(Excluding Trials 25-27)

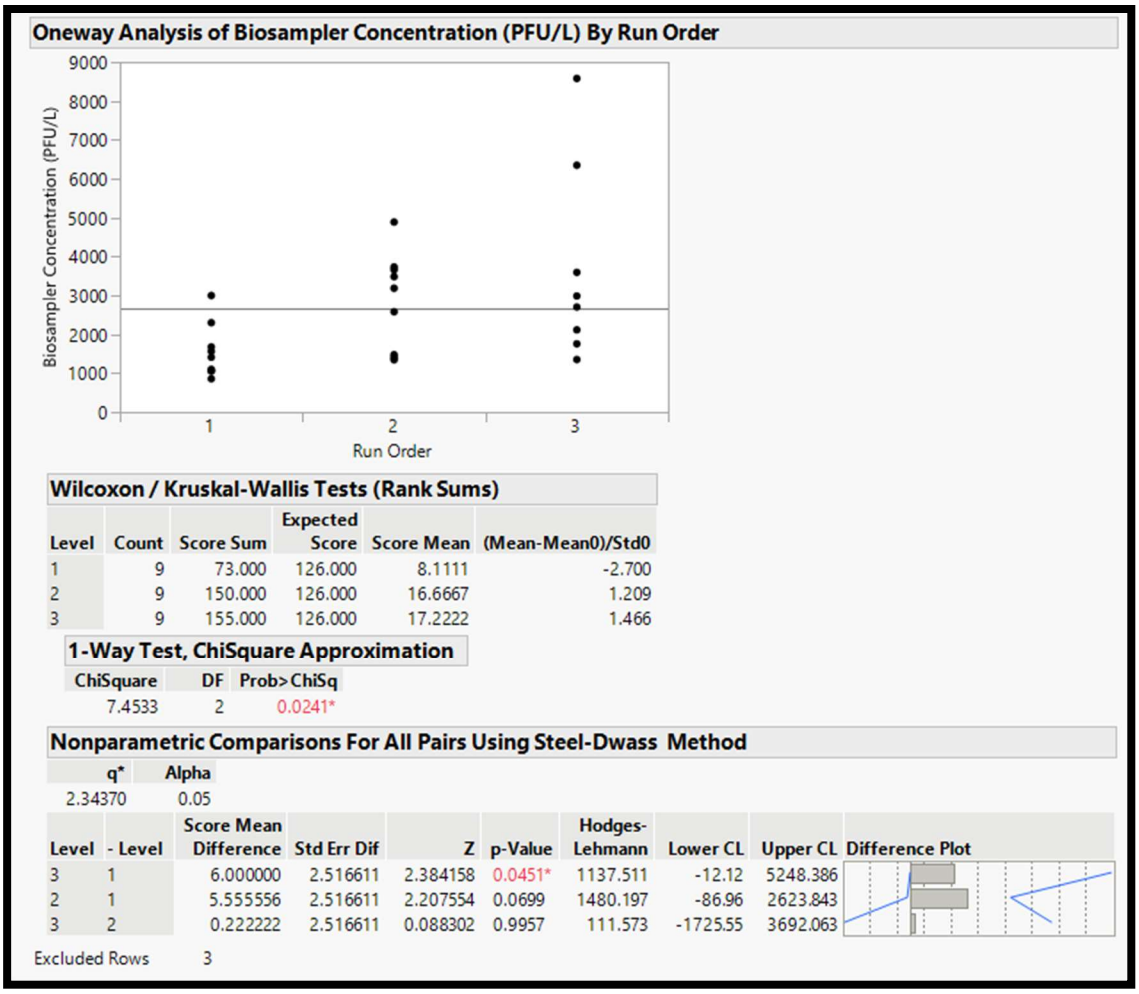

Figure L2. One-Way Analysis Biosampler® Concentration by Run Order (Excluding Trials 25-27)

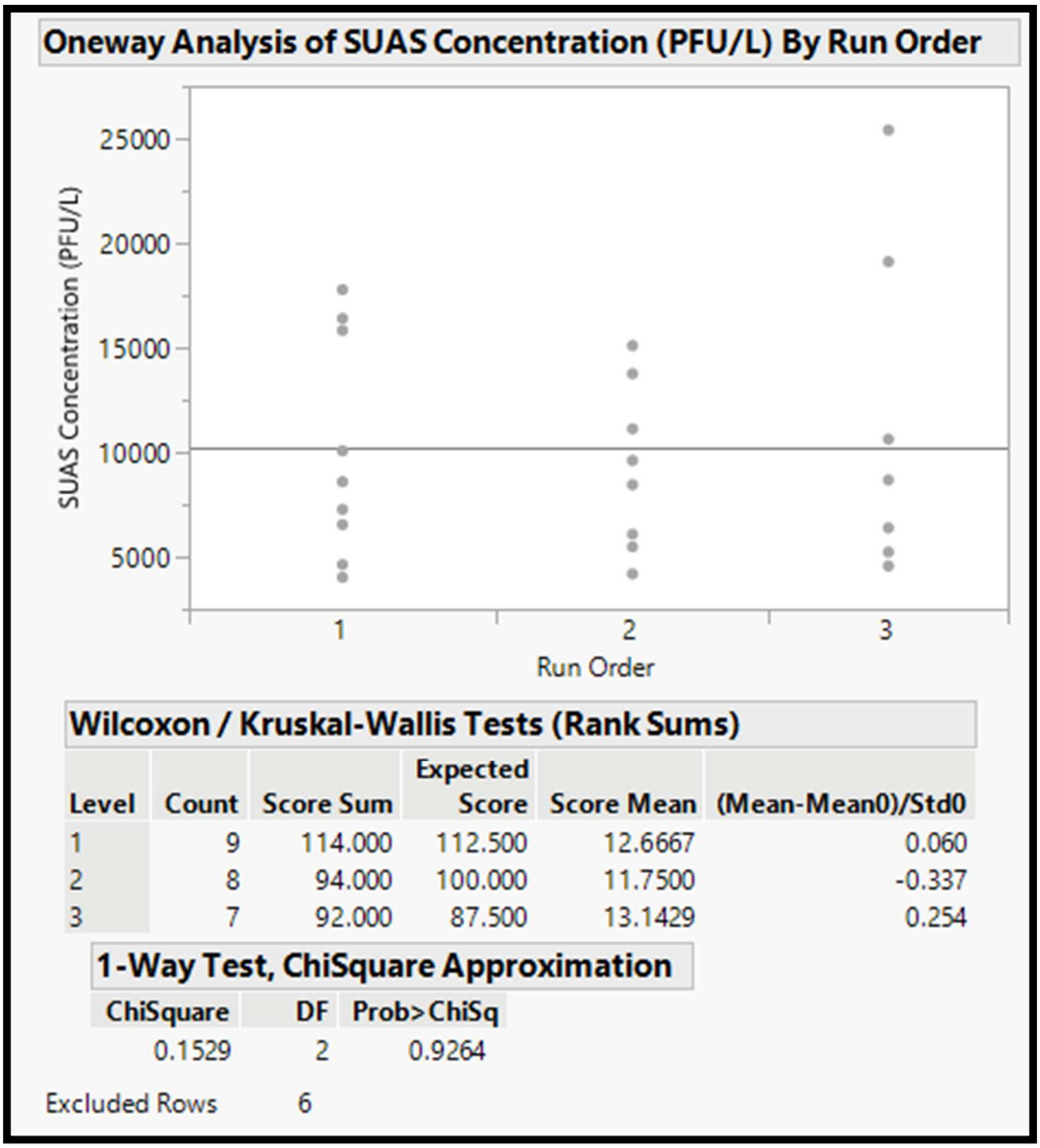

Figure L3. One-Way Analysis sUAS-Mounted Sampler Concentration by Run Order

(Excluding Trials 5, 6, 9, 25-27)

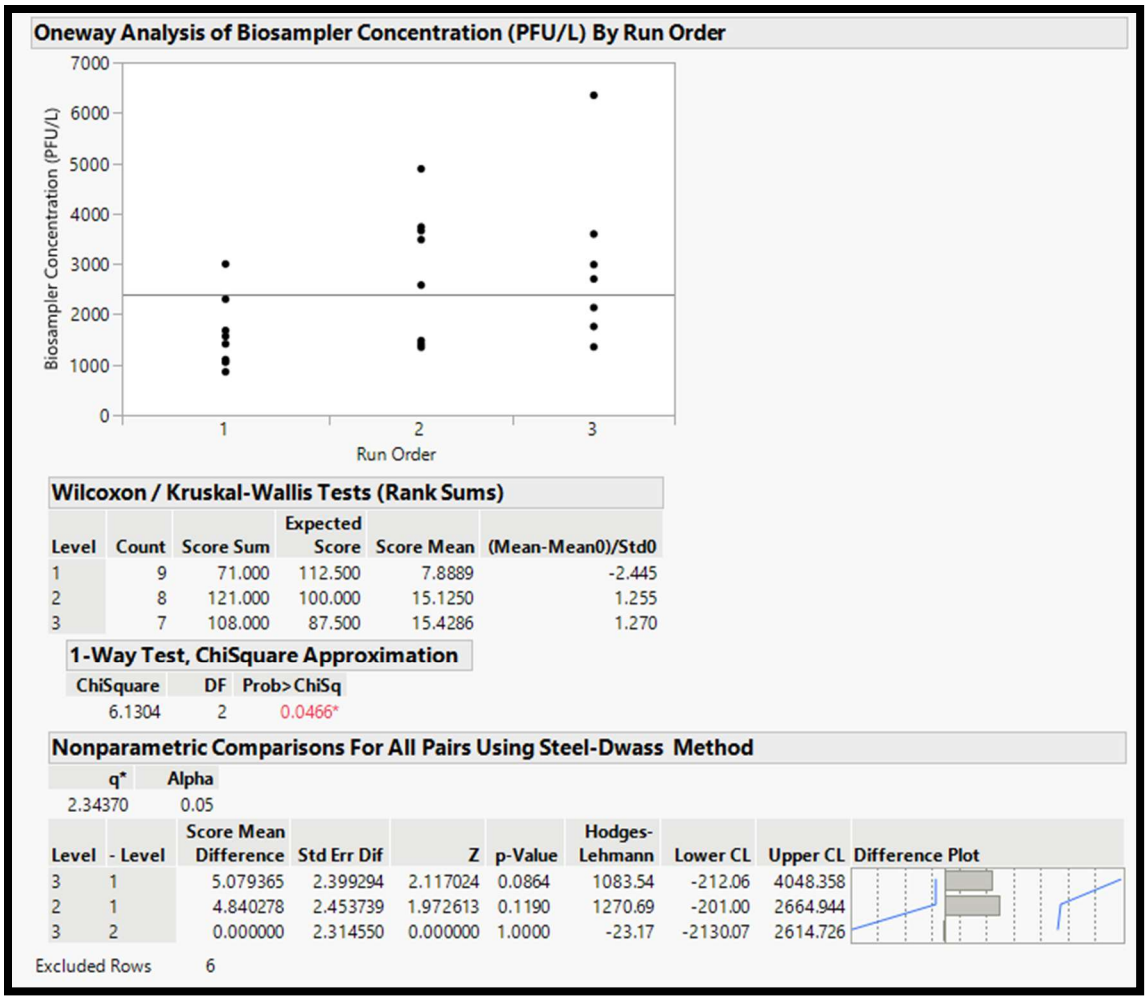

Figure L4. One-Way Analysis Biosampler® Concentration by Run Order (Excluding Trials 5, 6, 9, 25-27)

Bibliography

Adams, M. H. (1959). *Bacteriophages*. Interscience Publishers. https://archive.org/details/bacteriophages00adam/page/136/mode/2up.

American Conference of Governmental Industrial Hygienists (2022). TLVs and BEIs: Based on the Documentation of the Threshold Limit Values for Chemical Substances and Physical Agents & Biological Exposure Indices. Cincinnati, OH: ACGIH Signature Publications.

Anwar, D.; Oh, S.; Wu, C. (2010). Virus Collection Efficiency of Biosampler versus Impinger with Variable Time and Flow Rate (thesis). https://ufdcimages.uflib.ufl.edu/AA/00/06/11/34/00001/danwar-2010_04_21_Efficiency_of_BioSampler_vs_Impinger_Senior_Thesis_Diandra_Anwar.pdf.

Bałazy, A., Toivola, M., Adhikari, A., Sivasubramani, S. K., Reponen, T., & Grinshpun, S. A. (2006). Do N95 Respirators Provide 95% Protection Level Against Airborne Viruses, and How Adequate are Surgical Masks? *American Journal of Infection Control*, *34*(2), 51–57. https://doi.org/10.1016/J.AJIC.2005.08.018.

Brady, T. M., Strauch, A. L., Almaguer, C. M., Niezgoda, G., Shaffer, R. E., Yorio, P. L., & Fisher, E. M. (2017). Transfer of Bacteriophage MS2 and Fluorescein from N95 Filtering Facepiece Respirators to Hands: Measuring Fomite Potential. *Journal of Occupational and Environmental Hygiene*, *14*(11), 898. https://doi.org/10.1080/15459624.2017.1346799.

Burton, N. C., Grinshpun, S. A., & Reponen, T. (2007). Physical Collection Efficiency of Filter Materials for Bacteria and Viruses. *Annals of Occupational Hygiene*, *51*(2), 143. https://doi.org/10.1093/ANNHYG/MEL073.

Center for Disease Control and Prevention (2020). Biosafety in Microbiological and Biomedical Laboratories, 6th Ed. https://www.cdc.gov/labs/pdf/SF__19_308133-A_BMBL6_00-BOOK-WEB-final-3.pdf.

Chandler, J. C., Schaeffer, J. W., Davidson, M., Magzamen, S. L., Pérez-Méndez, A., Reynolds, S. J., Goodridge, L. D., Volckens, J., Franklin, A. B., Shriner, S. A., & Bisha, B. (2017). A Method for the Improved Detection of Aerosolized Influenza Viruses and the Male-Specific (F+) RNA Coliphage MS2. *Journal of Virological Methods*, *246*, 38–41. https://doi.org/10.1016/J.JVIROMET.2017.04.004.

Chapman, J. M. (2021). Re-Aerosolization of Dense Metal Oxide Simulating Radiological Contamination from Military Clothing (thesis). https://scholar.afit.edu/etd/4940/.

Chen, L., Lee, W. ju, Ma, Y., Jang, S. S., Fong, K., & Wang, S. (2022). The Efficacy of Different Sanitizers Against MS2 Bacteriophage Introduced onto Plastic or Stainless Steel Surfaces. *Current Research in Food Science*, *5*, 175–181. https://doi.org/10.1016/J.CRFS.2022.01.004.

Cooper, C. (2010). High Volume Air Sampling for Viral Aerosols: A Comparative Approach. *Theses and Dissertations*. https://scholar.afit.edu/etd/2125.

Cooper, C. W., Aithinne, K. A. N., Stevenson, B. S., Black, J. E., & Johnson, D. L. (2020). Comparison and Evaluation of a High Volume Air Sampling System for the Collection of Clostridioides difficile Endospore Aerosol in Health Care

Environments. *American Journal of Infection Control*, *48*(11), 1354–1360. https://doi.org/10.1016/J.AJIC.2020.04.014.

Cormier, J., & Janes, M. (2014). A Double Layer Plaque Assay Using Spread Plate Technique for Enumeration of Bacteriophage MS2. *Journal of Virological Methods*, *196*, 86–92. https://doi.org/10.1016/J.JVIROMET.2013.10.034.

Dawson, D. J., Paish, A., Staffell, L. M., Seymour, I. J., & Appleton, H. (2005). Survival of Viruses on Fresh Produce, Using MS2 as a Surrogate for Norovirus. *Journal of Applied Microbiology*, *98*(1), 203–209. https://doi.org/10.1111/J.1365-2672.2004.02439.X.

Dubovi Amn, E. J., & Akers, T. G. (1970). Airborne Stability of Tailless Bacterial Viruses S-13 and MS-2. *APPLIED MICROBIOLOGY*, *19*(4), 624–628.

Dybwad, M., Skogan, G., & Blatny, J. M. (2014). Comparative Testing and Evaluation of Nine Different Air Samplers: End-to-End Sampling Efficiencies as Specific Performance Measurements for Bioaerosol Applications. *Aerosol Science and Technology*, *48*(3), 282–295. https://doi.org/10.1080/02786826.2013.871501/SUPPL_FILE/UAST_A_871501_SM5434.ZIP.

Eninger, R. M., Adhikari, A., Reponen, T., Grinshpun, S. A., Hogan, C. J., & Biswas, P. (2009). Electrospray Versus Nebulization for Aerosolization and Filter Testing with Bacteriophage Particles. *Https://Doi-Org.Afit.Idm.Oclc.Org/10.1080/02786820802626355*, *43*(4), 298–304. https://doi.org/10.1080/02786820802626355.

Eninger, R. M., Honda, T., Adhikari, A., Heinonen-Tanski, H., Reponen, T., & Grinshpun, S. A. (2008). Filter Performance of N99 and N95 Facepiece Respirators Against Viruses and Ultrafine Particles. *Annals of Occupational Hygiene*, *52*(5), 385. https://doi.org/10.1093/ANNHYG/MEN019.

Eninger, R. M., & Johnson, R. L. (2015). Unmanned Aerial Systems in Occupational Hygiene—Learning from Allied Disciplines. *The Annals of Occupational Hygiene*, *59*(8), 949–958. https://doi.org/10.1093/ANNHYG/MEV041.

Environmental Protection Agency (2001). Method 1602: Male-specific (F+) and Somatic Coliphage in in Water by the Single Agar Layer (SAL) Procedure. https://www.epa.gov/sites/default/files/2015-12/documents/method_1602_2001.pdf.

Environmental Protection Agency (2018). Method 1643: Male-specific (F+) and Somatic Coliphage in Secondary (No Disinfection) Wastewater by the Single Agar Layer (SAL) Procedure. https://www.epa.gov/sites/default/files/2018-09/documents/method_1643_draft_2018.pdf#:~:text=This%20EPA%20method%20was%20developed%20to%20address%20stakeholder,disinfection%29%20wastewater%20samples%20for%20somatic%20and%20male-specific%20coliphage.

Fabian, P., McDevitt, J. J., Houseman, E. A., & Milton, D. K. (2009). Airborne Influenza Virus Detection with Four Aerosol Samplers Using Molecular and Infectivity Assays: Considerations for a New Infectious Virus Aerosol Sampler. *Indoor Air*, *19*(5), 433–441. https://doi.org/10.1111/J.1600-0668.2009.00609.X.

Fisher, E. M., Richardson, A. W., Harpest, S. D., Hofacre, K. C., & Shaffer, R. E. (2012). Reaerosolization of MS2 Bacteriophage from an N95 Filtering Facepiece Respirator

by Simulated Coughing. *The Annals of Occupational Hygiene*, *56*(3), 315–325. https://doi.org/10.1093/ANNHYG/MER101.

Fuller, S. (2022). Assessment of a Small Unmanned Aerial System (SUAS) Mounted Air Sampler for Collection of Bioaerosols Using *Bacillus thuringiensis* as a Surrogate for *Bacillus anthracis* (thesis).

Geoghegan, J. L., Pirotta, V., Harvey, E., Smith, A., Buchmann, J. P., Ostrowski, M., Eden, J. S., Harcourt, R., & Holmes, E. C. (2018). Virological Sampling of Inaccessible Wildlife with Drones. *Viruses*, *10*(6), E300–E300. https://doi.org/10.3390/V10060300.

Harvey, B. (2022) Evaluation of a Small Unmanned Aerial System (SUAS)-Based Air Sampler for the Collection of Vegetative Bacterial Aerosols (thesis).

Hedworth, H. A., Sayahi, T., Kelly, K. E., & Saad, T. (2021). The Effectiveness of Drones in Measuring Particulate Matter. *Journal of Aerosol Science*, *152*, 105702. https://doi.org/10.1016/J.JAEROSCI.2020.105702.

Hogan, C. J., Kettleson, E. M., Lee, M. H., Ramaswami, B., Angenent, L. T., & Biswas, P. (2005). Sampling Methodologies and Dosage Assessment Techniques for Submicrometre and Ultrafine Virus Aerosol Particles. *Journal of Applied Microbiology*, *99*(6), 1422–1434. https://doi.org/10.1111/J.1365-2672.2005.02720.X.

Hong, S., Bhardwaj, J., Han, C. H., & Jang, J. (2016). Gentle Sampling of Submicrometer Airborne Virus Particles Using a Personal Electrostatic Particle Concentrator. *Environmental Science and Technology*, *50*(22), 12365–12372. https://doi.org/10.1021/ACS.EST.6B03464.

Ibe, O. C. (2014). Introduction to Descriptive Statistics. *Fundamentals of Applied Probability and Random Processes*, 253–274. https://doi.org/10.1016/B978-0-12-800852-2.00008-0.

Jang, J., Bhardwaj, J., & Jang, J. (2022). Efficient Measurement of Airborne Viable Viruses Using the Growth-Based Virus Aerosol Concentrator with High Flow Velocities. *Journal of Hazardous Materials*, *434*, 128873. https://doi.org/10.1016/J.JHAZMAT.2022.128873.

Lenard, J. (2008). Viral Membranes. *Encyclopedia of Virology*, 308–314. https://doi.org/10.1016/B978-012374410-4.00530-6.

Leung, S. S. Y., Carrigy, N. B., Vehring, R., Finlay, W. H., Morales, S., Carter, E. A., Britton, W. J., Kutter, E., & Chan, H. K. (2019). Jet Nebulization of Bacteriophages with Different Tail Morphologies – Structural Effects. *International Journal of Pharmaceutics*, *554*, 322–326. https://doi.org/10.1016/J.IJPHARM.2018.11.026.

Li, X. B., Peng, Z. R., Lu, Q. C., Wang, D., Hu, X. M., Wang, D., Li, B., Fu, Q., Xiu, G., & He, H. (2020). Evaluation of Unmanned Aerial System in Measuring Lower Tropospheric Ozone and Fine Aerosol Particles Using Portable Monitors. *Atmospheric Environment*, *222*, 117134. https://doi.org/10.1016/J.ATMOSENV.2019.117134.

Lin, K., & Marr, L. C. (2017). Aerosolization of Ebola Virus Surrogates in Wastewater Systems. *Environmental Science and Technology*, *51*(5), 2669–2675. https://doi.org/10.1021/ACS.EST.6B04846/SUPPL_FILE/ES6B04846_SI_001.PDF.

Lin, K., Schulte, C. R., & Marr, L. C. (2020). Survival of MS2 and Φ6 Viruses in Droplets as a Function of Relative Humidity, Ph, and Salt, Protein, and Surfactant Concentrations. *PLOS ONE*, *15*(12), e0243505. https://doi.org/10.1371/JOURNAL.PONE.0243505.

Marintcheva, B. (2018). Introduction to Viral Structure, Diversity and Biology. *Harnessing the Power of Viruses*, 1–26. https://doi.org/10.1016/B978-0-12-810514-6.00001-5.

May, K. R. (1973). The Collison Nebulizer: Description, Performance and Application. *Journal of Aerosol Science*, *4*(3), 235–243. https://doi.org/10.1016/0021-8502(73)90006-2.

McCreedy, B. J. (1995). Detection of Viral Pathogens Using PCR Amplification. *Molecular Methods for Virus Detection*, 175–191. https://doi.org/10.1016/B978-012748920-9/50009-1.

Mullis, K. B., & Faloona, F. A. (1987). [21] Specific Synthesis of DNA in Vitro via a Polymerase-Catalyzed Chain Reaction. *Methods in Enzymology*, *155*(C), 335–350. https://doi.org/10.1016/0076-6879(87)55023-6.

Nayak, D. P. (2011). Virus Morphology, Replication, and Assembly. *Studies in Viral Ecology: Microbial and Botanical Host Systems*, *1*, 67–129. https://doi.org/10.1002/9781118025666.CH3.

Ohms, S. (2020). Development and Characterization of a Filter-Based Bioaerosol Development and Characterization of a Filter-Based Bioaerosol Sampler Capable of Integration into Small Unmanned Aerial Sampler Capable of Integration into Small

Unmanned Aerial Systems. Theses and Dissertations. 3249. https://scholar.afit.edu/etd/3249.

Olson, M. R., Axler, R. P., & Hicks, R. E. (2004). Effects of Freezing and Storage Temperature on MS2 Viability. *Journal of Virological Methods*, *122*(2), 147–152. https://doi.org/10.1016/J.JVIROMET.2004.08.010.

Occupational Health and Safety Administration, OSHA Technical Manual (OTM) Section II: Chapter 1 (2014). Retrieved November 8, 2022, from https://www.osha.gov/otm/section-2-health-hazards/chapter-1.

Palframan, M. C., Gruszewski, H. A., Schmale, D. G., & Woolsey, C. A. (2014). Detection of a Surrogate Biological Agent with a Portable Surface Plasmon Resonance Sensor Onboard an Unmanned Aircraft System. *Journal of Unmanned Vehicle Systems*, *2*(4), 103–118. https://doi.org/10.1139/JUVS-2013-0019.

Pirotta, V., Smith, A., Ostrowski, M., Russell, D., Jonsen, I. D., Grech, A., & Harcourt, R. (2017). An Economical Custom-Built Drone for Assessing Whale Health. *Frontiers in Marine Science*, *4*(DEC), 425. https://doi.org/10.3389/FMARS.2017.00425/BIBTEX.

Powers, C. W., Hanlon, R., Grothe, H., Prussin, A. J., Marr, L. C., & Schmale, D. G. (2018). Coordinated Sampling of Microorganisms over Freshwater and Saltwater Environments Using an Unmanned Surface Vehicle (USV) and a Small Unmanned Aircraft System (sUAS). *Frontiers in Microbiology*, *9*(AUG), 1668. https://doi.org/10.3389/FMICB.2018.01668/BIBTEX.

Ratnesar-Shumate, S., Pan, Y. le, Hill, S. C., Kinahan, S., Corson, E., Eshbaugh, J., & Santarpia, J. L. (2015). Fluorescence Spectra and Biological Activity of Aerosolized

Bacillus Spores and MS2 Bacteriophage Exposed to Ozone at Different Relative Humidities in a Rotating Drum. *Journal of Quantitative Spectroscopy and Radiative Transfer*, *153*, 13–28. https://doi.org/10.1016/J.JQSRT.2014.10.003.

Riemenschneider, L., Woo, M. H., Wu, C. Y., Lundgren, D., Wander, J., Lee, J. H., Li, H. W., & Heimbuch, B. (2010). Characterization of Reaerosolization from Impingers in an Effort to Improve Airborne Virus Sampling. *Journal of Applied Microbiology*, *108*(1), 315–324. https://doi.org/10.1111/J.1365-2672.2009.04425.X.

Rohi, G., Ejofodomi, O., & Ofualagba, G. (2020). Autonomous Monitoring, Analysis, and Countering of Air Pollution Using Environmental Drones. *Heliyon*, *6*(1), e03252. https://doi.org/10.1016/J.HELIYON.2020.E03252.

Sakurai, A., Nomura, N., Nanba, R., Sinkai, T., Iwaki, T., Obayashi, T., Hashimoto, K., Hasegawa, M., Sakoda, Y., Naito, A., Morizane, Y., Hosaka, M., Tsuboi, K., Kida, H., Kai, A., & Shibasaki, F. (2011). Rapid Typing of Influenza Viruses Using Super High-Speed Quantitative Real-Time PCR. *Journal of Virological Methods*, *178*(1–2), 75–81. https://doi.org/10.1016/J.JVIROMET.2011.08.015.

Sassi, H. P., Reynolds, K. A., Pepper, I. L., & Gerba, C. P. (2018). Evaluation of Hospital-Grade Disinfectants on Viral Deposition on Surfaces after Toilet Flushing. *American Journal of Infection Control*, *46*(5), 507–511. https://doi.org/10.1016/J.AJIC.2017.11.005.

Schuyler, T. J., & Guzman, M. I. (2017). Unmanned Aerial Systems for Monitoring Trace Tropospheric Gases. *Atmosphere 2017, Vol. 8, Page 206*, *8*(10), 206. https://doi.org/10.3390/ATMOS8100206.

Sigma-Aldrich. (2022). *Streptomycin Powder 3810-74-0*. https://www.sigmaaldrich.com/US/en/product/sial/s6501.

Su, Y., Wang, W., Wang, W., Zhai, L., Shen, X., Xu, J., & Li, Z. (2020). Re-Evaluation Of Biosampler and its Improvement for On-Line, Time-Resolved Monitoring of Environmental Coarse Aerosol. *Atmospheric Environment*, *225*, 117249. https://doi.org/10.1016/J.ATMOSENV.2019.117249.

Teunis, P. F. M., Lodder, W. J., Heisterkamp, S. H., & de Roda Husman, A. M. (2005). Mixed plaques: Statistical Evidence How Plaque Assays May Underestimate Virus Concentrations. *Water Research*, *39*(17), 4240–4250. https://doi.org/10.1016/J.WATRES.2005.08.012.

The White House (2022). National Biodefense Strategy and Implementation Plan. https://www.whitehouse.gov/wp-content/uploads/2022/10/National-Biodefense-Strategy-and-Implementation-Plan-Final.pdf.

Tseng, C. C., & Li, C. S. (2005). Collection Efficiencies of Aerosol Samplers for Virus-Containing Aerosols. *Journal of Aerosol Science*, *36*(5–6), 593–607. https://doi.org/10.1016/J.JAEROSCI.2004.12.004.

Tung-Thompson, G., Libera, D. A., Koch, K. L., III, F. L. de los R., & Jaykus, L.-A. (2015). Aerosolization of a Human Norovirus Surrogate, Bacteriophage MS2, during Simulated Vomiting. *PLOS ONE*, *10*(8), e0134277. https://doi.org/10.1371/JOURNAL.PONE.0134277.

Turgeon, N., Toulouse, M. J., Martel, B., Moineau, S., & Duchaine, C. (2014). Comparison of Five Bacteriophages as Models for Viral Aerosol Studies. *Applied*

and Environmental Microbiology, *80*(14), 4242–4250. https://doi.org/10.1128/AEM.00767-14.

United States, Department of the Air Force, Air Force Manual 10-2503, Operations in a Chemical, Biological, Radiological, and Nuclear Environment (2019). Retrieved from https://static.e-publishing.af.mil/production/1/af_a4/publication/afman10-2503/afman10-2503.pdf.

United States, Department of Defense, ATP 3-11.37: Multi-Service Tactics, Techniques, and Procedures for Chemical, Biological, Radiological, and Nuclear Sampling & Reconnaissance (2021). Retrieved from https://static.e-publishing.af.mil/production/1/af_a4/publication/afttp3-2.44/afttp3-2.44.pdf.

Verreault, D., Moineau, S., & Duchaine, C. (2008). Methods for Sampling of Airborne Viruses. *Microbiology and Molecular Biology Reviews : MMBR*, *72*(3), 413. https://doi.org/10.1128/MMBR.00002-08.

Willeke, K., Lin, X., & Grinshpun, S. A. (2007). Improved Aerosol Collection by Combined Impaction and Centrifugal Motion. *Aerosol Science and Technology* https://doi.org/10.1080/02786829808965536.

Wong, K., Bouchard, D., & Molina, M. (2014). Relative Transport of Human Adenovirus and MS2 in Porous Media. *Colloids and Surfaces B: Biointerfaces*, *122*, 778–784. https://doi.org/10.1016/J.COLSURFB.2014.08.020.

Zheng, Y., & Yao, M. (2017). Liquid Impinger Biosampler's Performance for Size-Resolved Viable Bioaerosol Particles. *Journal of Aerosol Science*, *106*, 34–42. https://doi.org/10.1016/J.JAEROSCI.2017.01.003.

Zuo, Z., Kuehn, T. H., Bekele, A. Z., Mor, S. K., Verma, H., Goyal, S. M., Raynor, P. C., & Pui, D. Y. H. (2014). Survival of Airborne MS2 Bacteriophage Generated from Human Saliva, Artificial Saliva, and Cell Culture Medium. *Applied and Environmental Microbiology*, *80*(9), 2796–2803. https://doi.org/10.1128/AEM.00056-14.

REPORT DOCUMENTATION PAGE

Form Approved
OMB No. 074-0188

1. REPORT DATE *(DD-MM-YYYY)*	2. REPORT TYPE	3. DATES COVERED *(From – To)*
23-03-2023	Master's Thesis	August 2021 – March 2023

TITLE AND SUBTITLE
A COMPARATIVE ANALYSIS OF VIRAL AEROSOL BIOLOGICAL SAMPLING EFFICIENCY OF A SMALL UNMANNED AIRCRAFT SYSTEM (SUAS)-MOUNTED AEROSOL SAMPLER AND A REFERENCE STATIC BIOSAMPLER®

5a. CONTRACT NUMBER

5b. GRANT NUMBER
20-004

5c. PROGRAM ELEMENT NUMBER

6. AUTHOR(S)
Moroz, Jonathan D., Master Sergeant, USAF

5d. PROJECT NUMBER
21V230

5e. TASK NUMBER

5f. WORK UNIT NUMBER

7. PERFORMING ORGANIZATION NAMES(S) AND ADDRESS(S)
Air Force Institute of Technology
Graduate School of Engineering and Management (AFIT/ENV)
2950 Hobson Way, Building 640
WPAFB OH 45433-8865

8. PERFORMING ORGANIZATION REPORT NUMBER
AFIT-ENV-MS-23-M-215

9. SPONSORING/MONITORING AGENCY NAME(S) AND ADDRESS(ES)
711 Human Performance Wing (USAFSAM/FESS)
2510 Fifth Street, Wright-Patterson AFB, OH 45433
(937) 938- 3761
ATTN: Ronald Riegle; ronald.riegle.1.ctr@us.af.mil

10. SPONSOR/MONITOR'S ACRONYM(S)
USAFSAM/RHBAF

11. SPONSOR/MONITOR'S REPORT NUMBER(S)

12. DISTRIBUTION/AVAILABILITY STATEMENT
DISTRUBTION STATEMENT A. APPROVED FOR PUBLIC RELEASE; DISTRIBUTION UNLIMITED

13. SUPPLEMENTARY NOTES

14. ABSTRACT

Bioaerosol sampling using small unmanned aerial systems (sUAS) is a rapidly developing field that may result in a paradigm shift in emergency response and industrial hygiene sampling conventions. These technologies offer decreased sample acquisition times, larger sampling area coverage, and reduced health and safety risks to traditional human sampling teams. This potential requires a comprehensive investigation of sUAS capabilities and limitations. This study is a continuation of the characterization of an AFIT-developed sUAS-mounted aerosol sampler, proven capable of collecting viable vegetative and spore-forming bacteria through previous AFIT research. Within this study, viral biological sampling efficiency (BSE) of the sUAS-mounted aerosol sampler affixed with SKC 37 mm gelatin filter media is compared to a reference SKC Biosampler®, using Male Specific Coliphage 2 (MS2) as a model viral organism. Experimental trials were conducted within a 5.35 cubic meter, controlled aerosol test chamber using a 6-jet Collison nebulizer to loft viral aerosols. Plaque assay analysis was used to enumerate sampled MS2. Results of this study determined the mean relative BSE of the sUAS-mounted aerosol sampler to the Biosampler® in the collection of viable MS2 bacteriophage per liter of air sampled to be 4.98 (95% CI 3.9, 6.1), under these experimental conditions.

15. SUBJECT TERMS
CBRN, small unmanned aircraft system, sUAS, bioaerosol, MS2 bacteriophage, air sampling, viral aerosol

16. SECURITY CLASSIFICATION OF:			17. LIMITATION OF ABSTRACT	18. NUMBER OF PAGES	19a. NAME OF RESPONSIBLE PERSON
a. REPORT	b. ABSTRACT	c. THIS PAGE			Dr. Jeremy Slagley, AFIT/ENV
U	U	U	UU	117	19b. TELEPHONE NUMBER *(Include area code)* (937) 255-3636, ext. 4632 (Jeremy.slagley@afit.edu)

Standard Form 298 (Rev. 8-98)
Prescribed by ANSI Std. Z39-18